Deciphering the Structure of Gaseous Detonations by Numerical Simulation

Ralf Deiterding
Computer Science and Mathematics Division
Oak Ridge National Laboratory

6th Annual Symposium of the Burgers Program for Fluid Dynamics
University of Maryland, College Park, Nov 18, 2009

Work supported by DFG high priority research program “Analysis and Numerics of Conservation Laws”, grant Ba 840/3-3 and currently sponsored by the Office of Advanced Scientific Computing Research; U.S. Department of Energy (DOE) and was performed at the Oak Ridge National Laboratory, which is managed by UT-Battelle, LLC under Contract No. DE-AC05-00OR22725.

Outline of the talk

- Computational approach
  - *Introduction*
  - *Governing equations*
  - *Finite volume method*
    - *Upwind scheme, embedded boundaries*
    - *Dynamic mesh adaptation, parallelization*
  - *Shock-induced combustion examples*
- Mach reflection patterns in detonations
  - *Qualitative description*
  - *Shock polar analysis for triple points in detonations*
    - *Oblique shock relations for real gases*
    - *Reflection type transition criteria*
    - *Construction of a transition diagram for low-pressure H_2:O_2:Ar*
  - *Weak and strong structures in detonations in 2D pipe bends*
    - *Classification of observed Mach reflection structures*
- Short outlook: comparison 2D vs. 3D
- Conclusions

Difficulties in detonation simulations

1. Discontinuous solutions $\rightarrow$ high-resolution finite volume method with upwinding in all characteristic fields
2. Stiffness of reaction terms, $\Delta t_c << \Delta t \rightarrow$ Numerical decoupling of time operators with method of fractional steps and local time steps Δt_c
3. Extremely high spatial resolution in reaction zone necessary. Discretization of an exact ZND detonation:

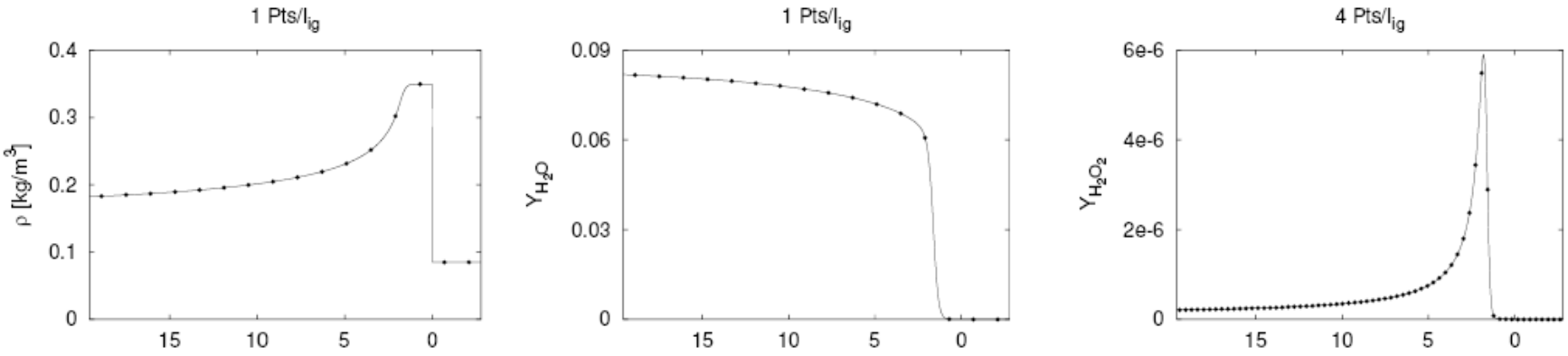

minimal spatial resolution: 7 − 8 Pts/l_{ig} $\rightarrow \Delta x \approx 0.2 - 0.175$mm

Uniform grids for typical geometries: > 10^7 Pts in 2D, > 10^9 Pts in 3D $\rightarrow$ Self-adaptive finite volume method (AMR)

4. Problem size even with AMR in 3D enormous $\rightarrow$ parallelization for massively parallel systems with distributed memory

Hydrodynamic equations

Euler equations for mixtures

$$\frac{\partial \rho}{\partial t} + \frac{\partial}{\partial x_k}(\rho u_k) = 0$$

$$\frac{\partial}{\partial t}(\rho u_i) + \frac{\partial}{\partial x_k}(\rho u_i u_k + \delta_{ik} p) = 0$$

$$\frac{\partial E}{\partial t} + \frac{\partial}{\partial x_k}(u_k(E+p)) = 0$$

$$\frac{\partial}{\partial t}(\rho Y_i) + \frac{\partial}{\partial x_k}(\rho Y_i u_k) = \dot{m}_i$$

Implicit equation of state

$$\rho h - p - E + \frac{1}{2}\rho u_k u_k = 0$$

Ideal gas law

$$p = \rho \mathcal{R} T \sum_{i=1}^{N} \frac{Y_i}{W_i}$$

Caloric equation

$$h = \sum_{i=1}^{N} h_i(T) Y_i \qquad \text{with}$$

$$h_i(T) = h_i^0 + \int_{T^0}^{T} c_{pi}(T^*) dT^*$$

Chemical kinetics with Arrhenius law

$$\dot{m}_i = W_i \sum_{j=1}^{M} (\nu_{ji}^r - \nu_{ji}^f)[k_j^f \prod_{n=1}^{N} (\frac{\rho_n}{W_n})^{\nu_{jn}^f} - k_j^r \prod_{n=1}^{N} (\frac{\rho_n}{W_n})^{\nu_{jn}^r}]$$

Finite volume scheme

- Method of fractional steps

$$\mathcal{H}^{(\Delta t)}: \quad \partial_t \mathbf{q} + \nabla \cdot \mathbf{f}(\mathbf{q}) = 0\,, \quad \text{IC: } \mathbf{Q}(t_m) \overset{\Delta t}{\Longrightarrow} \tilde{\mathbf{Q}}$$

$$\mathcal{S}^{(\Delta t)}: \quad \partial_t \mathbf{q} = \mathbf{s}(\mathbf{q})\,, \quad \text{IC: } \tilde{\mathbf{Q}} \overset{\Delta t}{\Longrightarrow} \mathbf{Q}(t_m + \Delta t)$$

1st-order: $\mathbf{Q}(t_m + \Delta t) = \mathcal{S}^{(\Delta t)} \mathcal{H}^{(\Delta t)}(\mathbf{Q}(t_m))$

2nd-order: $\mathbf{Q}(t_m + \Delta t) = \mathcal{S}^{(\frac{1}{2}\Delta t)} \mathcal{H}^{(\Delta t)} \mathcal{S}^{(\frac{1}{2}\Delta t)}(\mathbf{Q}(t_m))$

- Hydrodynamics
  - *Extension to 2d and 3d via dimensional splitting*
  - *Linearized Riemann-solver of Roe-type for thermally perfect gas-mixtures (Grossman, Cinella, J. Comput. Phys. 85, 1990)*
  - *Positivity-preserving*
    - *Switching to HLL for unphysical ρ, p*
    - *Fix for Y_i (Larrouturou, J. Comput. Phys. 95, 1991).*
  - *Entropy fix modification to avoid carbuncle phenomenon (Sanders, Morano, Druguett, J. Comput. Phys. 145, 1998)*
  - *2nd-order MUSCL reconstruction*
- Evaluation of T with Newton iteration / bisection

RD, G. Bader, Analysis and Numerics for Conservation Laws, p. 69-91, Springer, 2005

Reaction mechanism

- 4th-order semi-implicit Rosen-brock-Wanner ODE solver with stepsize adjustment
- Production rates evaluated with automatically generated F77 function (4x faster Chemkin)
- Jacobian approximated
- c_{pi}, h_i tabulated
- All subsequent computations for hydrogen-oxygen mechanism with 34 elementary reaction, 9 species O_2, H_2, H_2O, H, O, OH, HO_2, H_2O_2, Ar

				A [cm, mol, s]	β	E_{act} [cal mol^{-1}]
1.	$H + O_2$	$\longrightarrow$	$O + OH$	1.86×10^{14}	0.00	16790.
2.	$O + OH$	$\longrightarrow$	$H + O_2$	1.48×10^{13}	0.00	680.
3.	$H_2 + O$	$\longrightarrow$	$H + OH$	1.82×10^{10}	1.00	8900.
4.	$H + OH$	$\longrightarrow$	$H_2 + O$	8.32×10^{09}	1.00	6950.
5.	$H_2O + O$	$\longrightarrow$	$OH + OH$	3.39×10^{13}	0.00	18350.
6.	$OH + OH$	$\longrightarrow$	$H_2O + O$	3.16×10^{12}	0.00	1100.
7.	$H_2O + H$	$\longrightarrow$	$H_2 + OH$	9.55×10^{13}	0.00	20300.
8.	$H_2 + OH$	$\longrightarrow$	$H_2O + H$	2.19×10^{13}	0.00	5150.
9.	$H_2O_2 + OH$	$\longrightarrow$	$H_2O + HO_2$	1.00×10^{13}	0.00	1800.
10.	$H_2O + HO_2$	$\longrightarrow$	$H_2O_2 + OH$	2.82×10^{13}	0.00	32790.
11.	$HO_2 + O$	$\longrightarrow$	$OH + O_2$	5.01×10^{13}	0.00	1000.
12.	$OH + O_2$	$\longrightarrow$	$HO_2 + O$	6.46×10^{13}	0.00	56160.
13.	$HO_2 + H$	$\longrightarrow$	$OH + OH$	2.51×10^{14}	0.00	1900.
14.	$OH + OH$	$\longrightarrow$	$HO_2 + H$	1.20×10^{13}	0.00	40100.
15.	$HO_2 + H$	$\longrightarrow$	$H_2 + O_2$	2.51×10^{13}	0.00	700.
16.	$H_2 + O_2$	$\longrightarrow$	$HO_2 + H$	5.50×10^{13}	0.00	57800.
17.	$HO_2 + OH$	$\longrightarrow$	$H_2O + O_2$	5.01×10^{13}	0.00	1000.
18.	$H_2O + O_2$	$\longrightarrow$	$HO_2 + OH$	6.31×10^{14}	0.00	73860.
19.	$H_2O_2 + O_2$	$\longrightarrow$	$HO_2 + HO_2$	3.98×10^{13}	0.00	42640.
20.	$HO_2 + HO_2$	$\longrightarrow$	$H_2O_2 + O_2$	1.00×10^{13}	0.00	1000.
21.	$H_2O_2 + H$	$\longrightarrow$	$HO_2 + H_2$	1.70×10^{12}	0.00	3750.
22.	$HO_2 + H_2$	$\longrightarrow$	$H_2O_2 + H$	7.24×10^{11}	0.00	18700.
23.	$H_2O + M$	$\longrightarrow$	$H + OH + M$	2.19×10^{16}	0.00	105000.
24.	$H + OH + M$	$\longrightarrow$	$H_2O + M$	1.41×10^{23}	−2.00	0.
25.	$H + O_2 + M$	$\longrightarrow$	$HO_2 + M$	1.66×10^{15}	0.00	−1000.
26.	$HO_2 + M$	$\longrightarrow$	$H + O_2 + M$	2.29×10^{15}	0.00	45900.
27.	$H_2O_2 + M$	$\longrightarrow$	$OH + OH + M$	1.20×10^{17}	0.00	45500.
28.	$OH + OH + M$	$\longrightarrow$	$H_2O_2 + M$	9.12×10^{14}	0.00	−5070.
29.	$O + H + M$	$\longrightarrow$	$OH + M$	1.00×10^{16}	0.00	0.
30.	$OH + M$	$\longrightarrow$	$O + H + M$	7.94×10^{19}	−1.00	103720.
31.	$O_2 + M$	$\longrightarrow$	$O + O + M$	5.13×10^{15}	0.00	115000.
32.	$O + O + M$	$\longrightarrow$	$O_2 + M$	4.68×10^{15}	−0.28	0.
33.	$H_2 + M$	$\longrightarrow$	$H + H + M$	2.19×10^{14}	0.00	96000.
34.	$H + H + M$	$\longrightarrow$	$H_2 + M$	3.02×10^{15}	0.00	0.

Third body efficiencies: $f(O_2) = 0.40$, $f(H_2O) = 6.50$

C. K. Westbrook. Chemical kinetics of hydrocarbon oxidation in gaseous detonations. *J. Combustion and Flame*, 46:191–210, 1982.

Detonation ignition in a shock tube

- Shock-induced detonation ignition of $H_2 : O_2 : Ar/2 : 1 : 7$ in a 1d shock tube closed at the left end, domain simulated: 12 cm
- Insufficient resolution leads to inaccurate results
- Reflected shock is captured by the FV scheme correctly at all resolutions, but the detonation is resolution-dependent

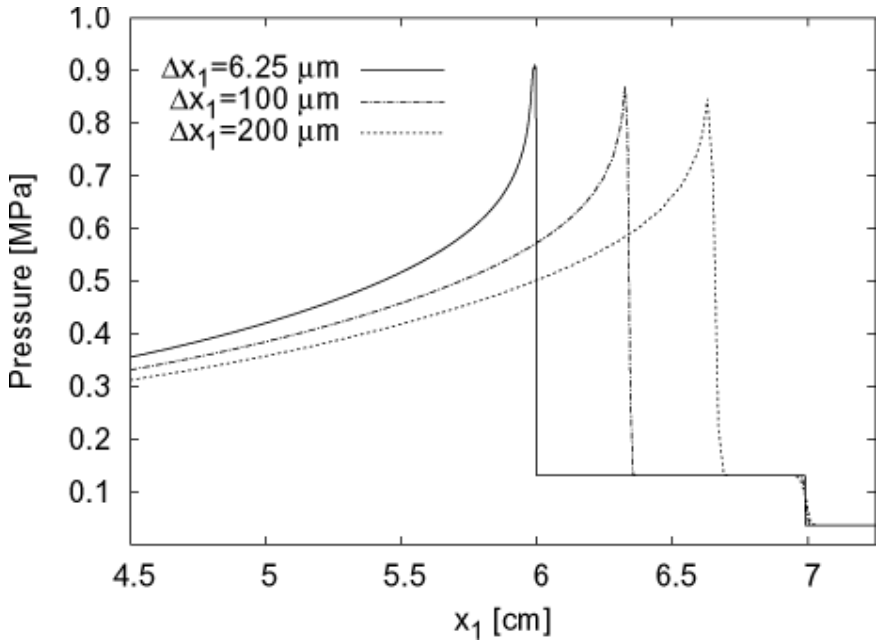

Δx_1=100 μm

Δx_1=6.25 μm

Analysis of configuration in Oran et al., J. Combust. Flame, 48:135–148, 1982

Detonation ignition in a shock tube

- Shock-induced detonation ignition of $H_2 : O_2 : Ar/2 : 1 : 7$ in a 1d shock tube closed at the left end, domain simulated: 12 cm
- Insufficient resolution leads to inaccurate results
- Reflected shock is captured by the FV scheme correctly at all resolutions, but the detonation is resolution-dependent

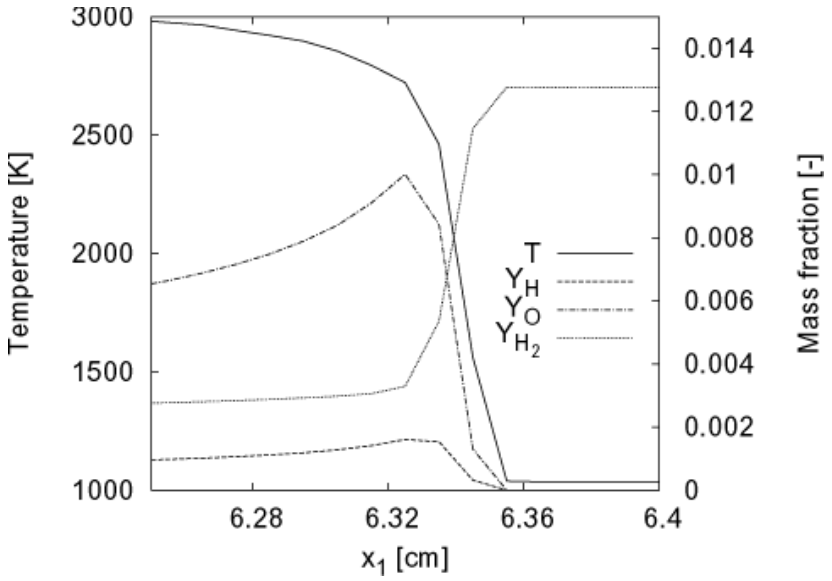

Δx_1=100 μm

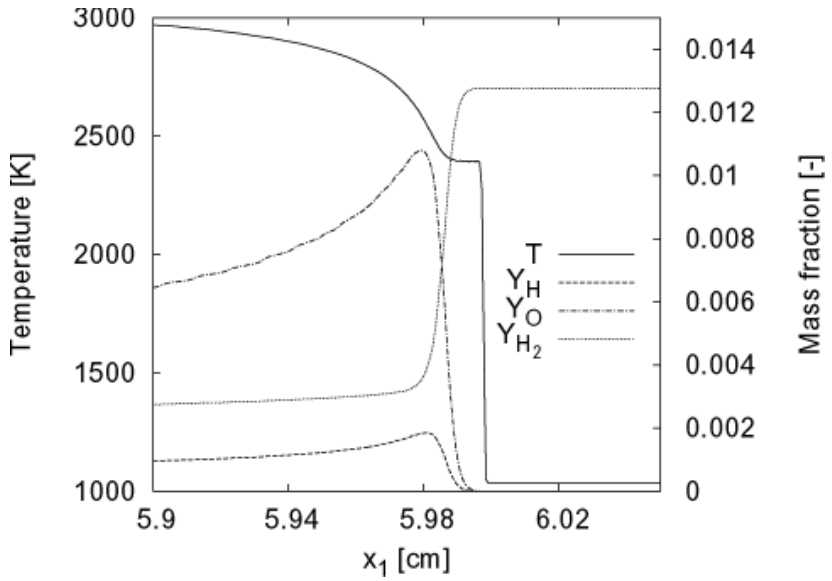

Δx_1=6.25 μm

Analysis of configuration in Oran et al., J. Combust. Flame, 48:135–148, 1982

Structured AMR for hyperbolic problems

- Refined subgrids overlay coarser ones
- Computational decoupling of subgrids by using ghost cells
- Refinement in space *and* time
- Block-based data structures
- Cells without mark are refined
- Cluster-algorithm necessary
- Efficient cache-reuse / vectorization possible
- Discretization

$$\mathbf{Q}_{jk}^{n+1} = \mathbf{Q}_{jk}^{n} - \frac{\Delta t}{\Delta x_1}\left[\mathbf{F}^1_{j+\frac{1}{2},k} - \mathbf{F}^1_{j-\frac{1}{2},k}\right] - \frac{\Delta t}{\Delta x_2}\left[\mathbf{F}^2_{j,k+\frac{1}{2}} - \mathbf{F}^2_{j,k-\frac{1}{2}}\right]$$

is applied patch-wise

$\rightarrow$ Inherently parallel approach

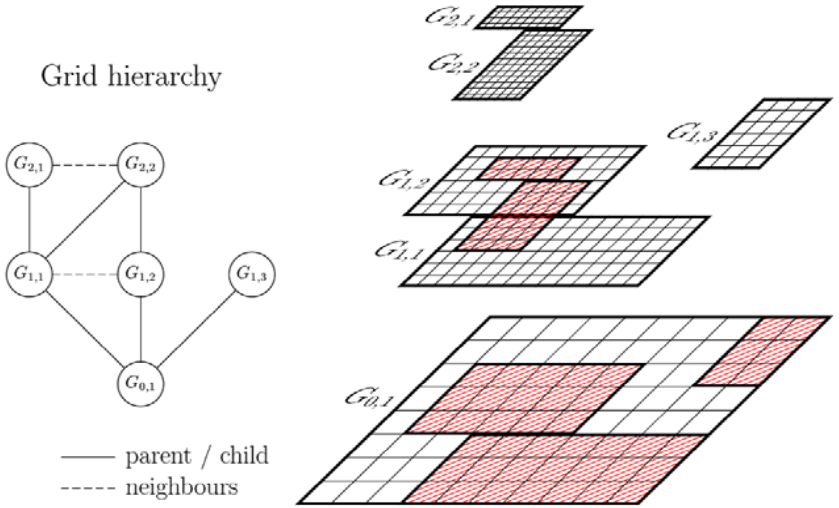

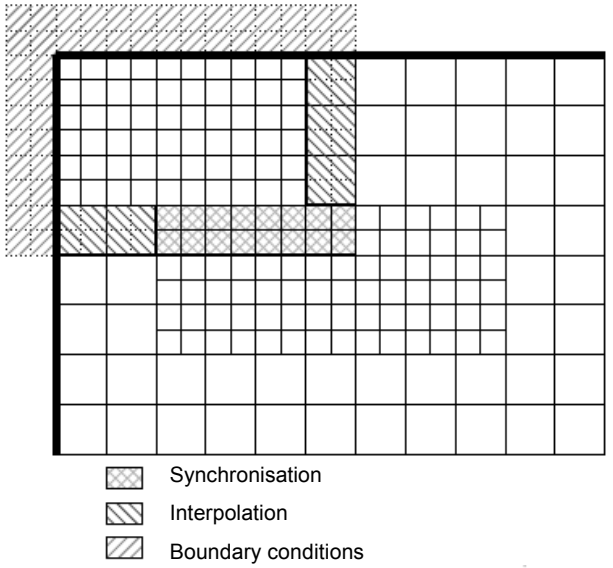

M. Berger and P. Colella, J. Comput. Phys. 82, 1988

Parallelization strategy

- Data of all levels resides on same node → Interpolation and averaging remain strictly local
- Only parallel operations to be considered:
  - *Parallel synchronization as part of ghost cell setting*
  - *Load-balanced repartitioning of data blocks as part of* **`Regrid(l)`**
  - *Application of flux correction terms on coarse-grid cells*
- Partitioning at root level with generalized Hilbert space-filling curve defined in AMR index coordinate system by M. Parashar

$$\mathcal{W}(\Omega) = \sum_{l=0}^{l_{\max}} \left[\mathcal{N}_l(G_l \cap \Omega) \prod_{\nu=0}^{l} r_\nu \right]$$

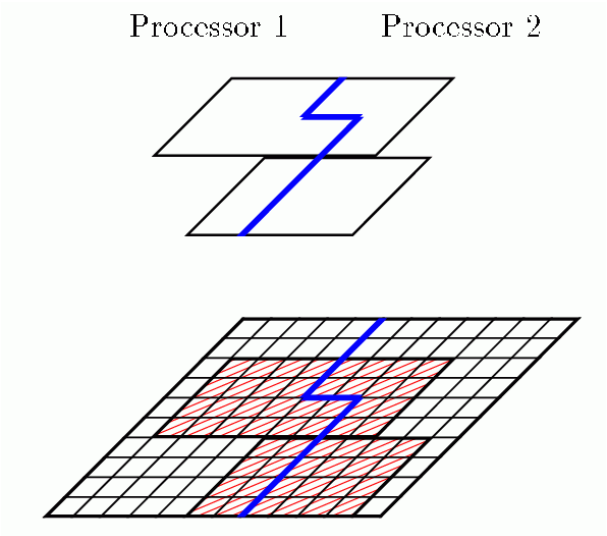

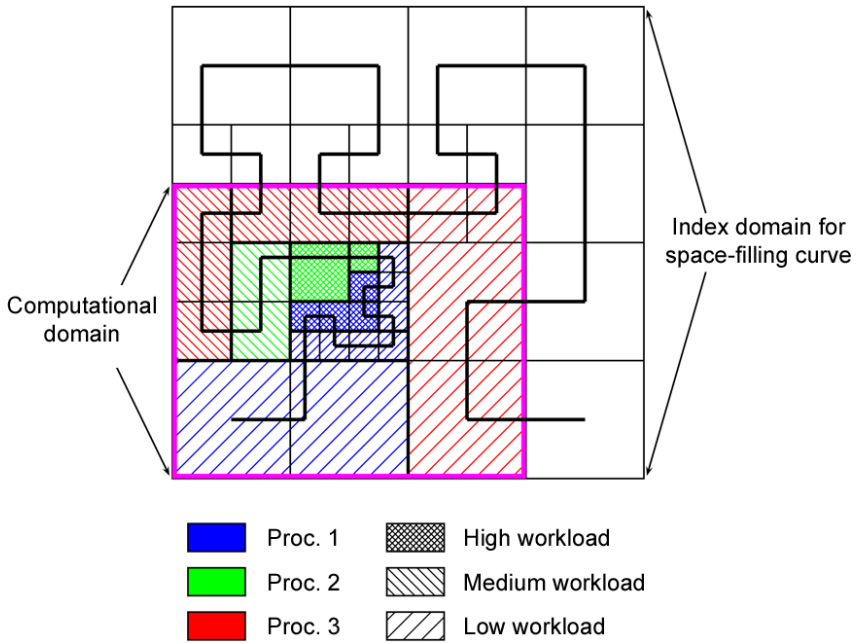

Embedded boundary method

- Incorporate complex moving boundary/ interfaces into a Cartesian solver (extension of work by R.Fedkiw and T.Aslam)
- Implicit boundary representation via distance function φ, normal $n = \nabla\varphi / |\nabla\varphi|$
- Treat an interface as a moving rigid wall
- Method diffuses boundary and is therefore not conservative
- Construction of values in embedded boundary cells by interpolation / extrapolation

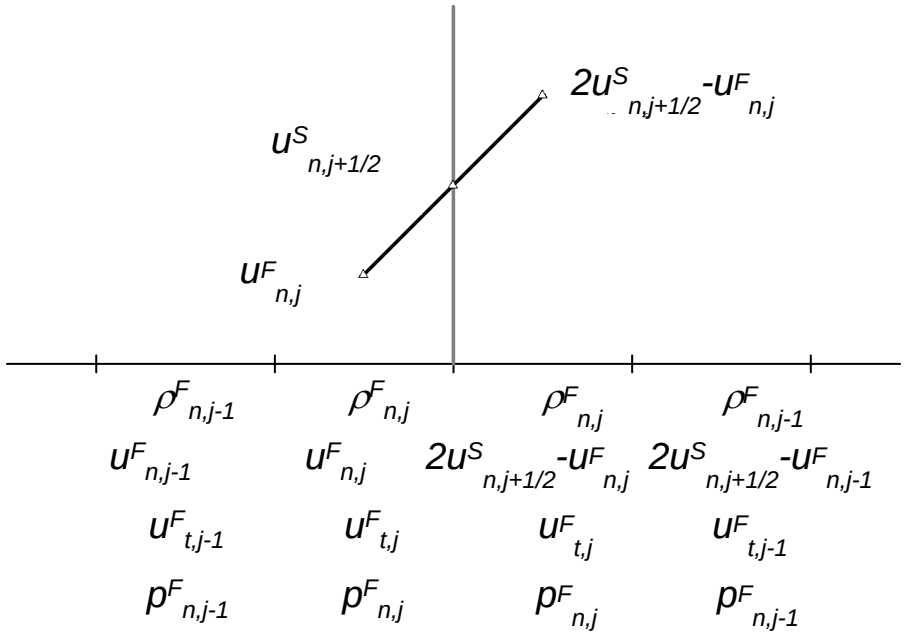

Velocity: $\boldsymbol{u}^F_{Gh} = 2((\boldsymbol{u}^S - \boldsymbol{u}^F_M)\cdot \boldsymbol{n})\,\boldsymbol{n} + \boldsymbol{u}^F_M$

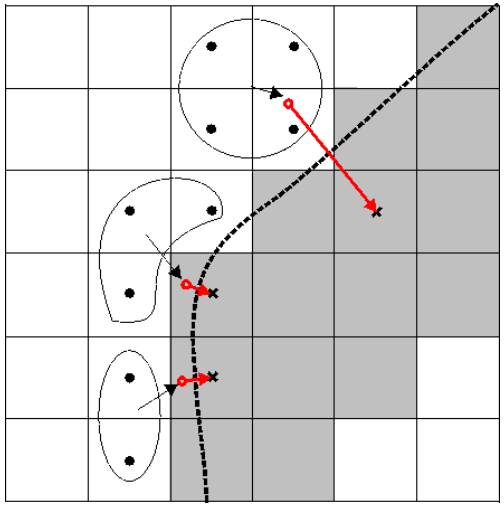

- Higher resolution at embedded boundary required than with first-order unstructured scheme
- Appropriate level-set-based refinement criteria are available to cure deficiencies

RD, Computers & Structures, 87: 769-783, 2009

Shock-induced combustion around a sphere

- Spherical projectile of radius 1.5 mm travels with constant velocity v_l=2170.6 m/s through H_2 : O_2 : Ar/2:1:7 at 6.67 kPa and T=298 K
- Cylindrical symmetric simulation on AMR base mesh of 70x40 cells
- Comparison in quasi-steady state at t=350 μs

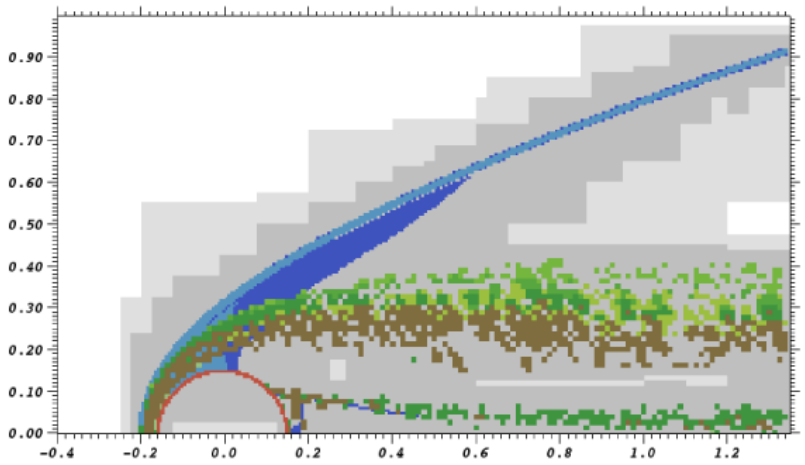

Refinement indicators on level 3

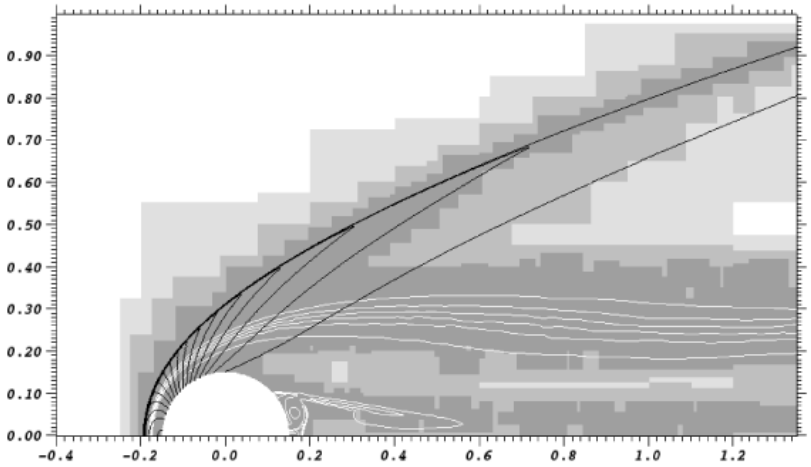

4-level with factors 2,2,4 (~19 Pts/l_{ig})

Setup from P. Hung, PhD thesis, GalCIT, 2003

Shock-induced combustion around a sphere

- Spherical projectile of radius 1.5 mm travels with constant velocity v_l=2170.6 m/s through H_2 : O_2 : Ar/2:1:7 at 6.67 kPa and T=298 K
- Cylindrical symmetric simulation on AMR base mesh of 70x40 cells
- Comparison in quasi-steady state at t=350 μs

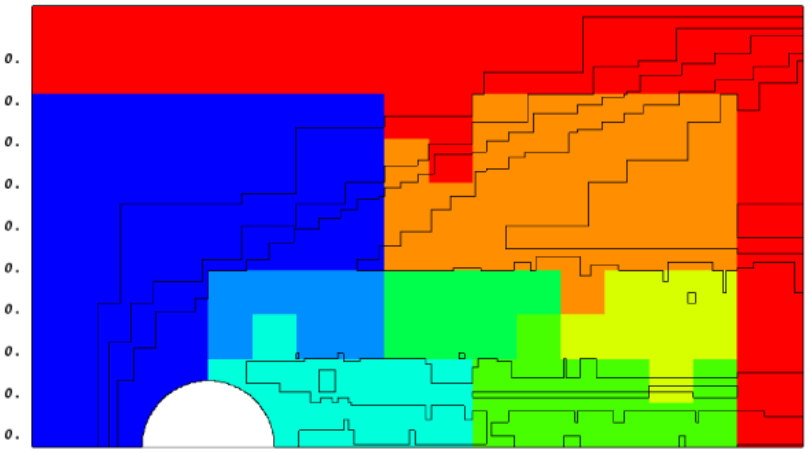

Distribution to 8 processors

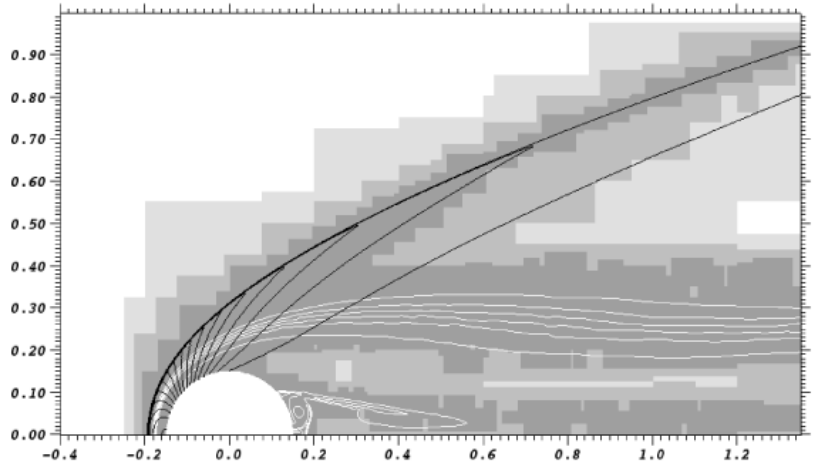

4-level with factors 2,2,4 (~19 Pts/l_{ig})

Setup from P. Hung, PhD thesis, GalCIT, 2003

Transverse detonation structure - Regular instability

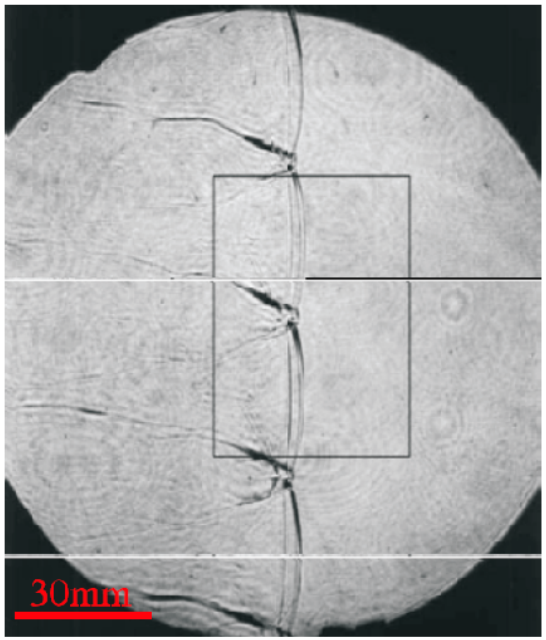

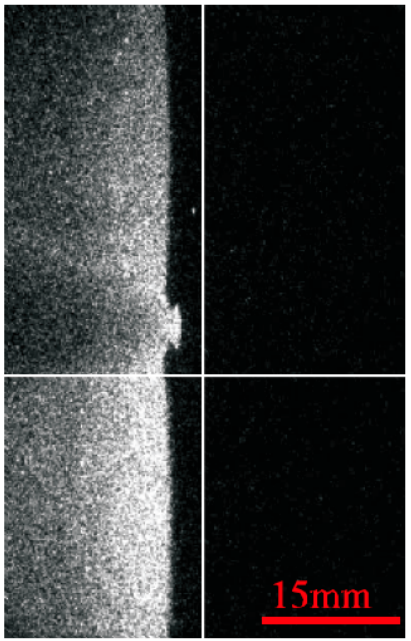

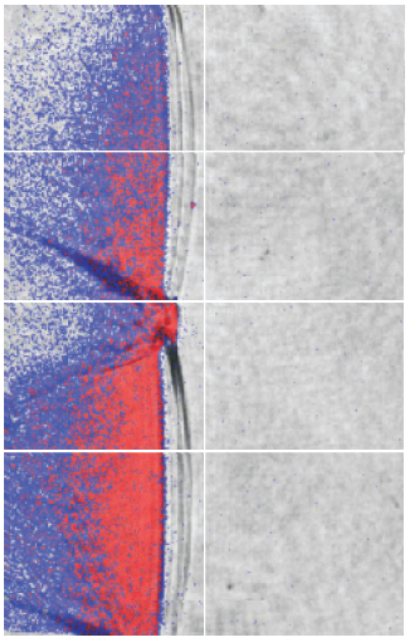

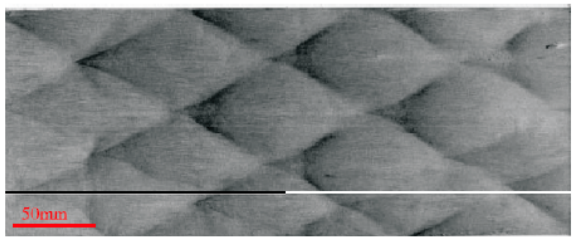

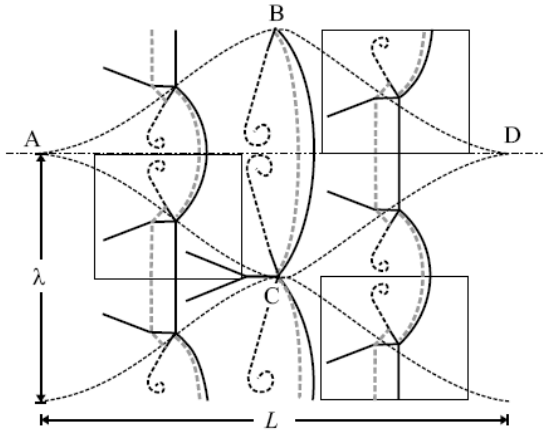

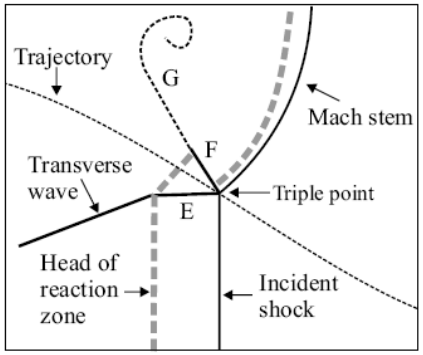

E: Reflected shock. F: Slip line. G: Diffusive extension of slip line.

Photo courtesy: J. Austen, F. Pintgen, J.E. Shepherd (GalCIT)

Simulation of regular cellular structures

- Regular Chapman-Jouguet detonation for $H_2 : O_2 : Ar/2 : 1 : 7$ at T_0 = 298K and p_0 = 10 kPa, cell width 1.6 cm.
- Perturb 1d solution with unreacted high-pressure pocket behind front
- Triple point trajectories by tracking max$|\omega|$ on auxiliary mesh

$$\omega = \frac{\partial u_2}{\partial x_1} - \frac{\partial u_1}{\partial x_2}$$

- Adaptation criteria:
  - *Scaled gradients of ρ and p*
  - *Error estimation in Y_i by Richardson extrapolation*
- 67.6 Pts within induction length. 4 additional refinement levels (2,2,2,4).
- Similar configuration as E. Oran et al., J. Combustion and Flame 113, 1998.

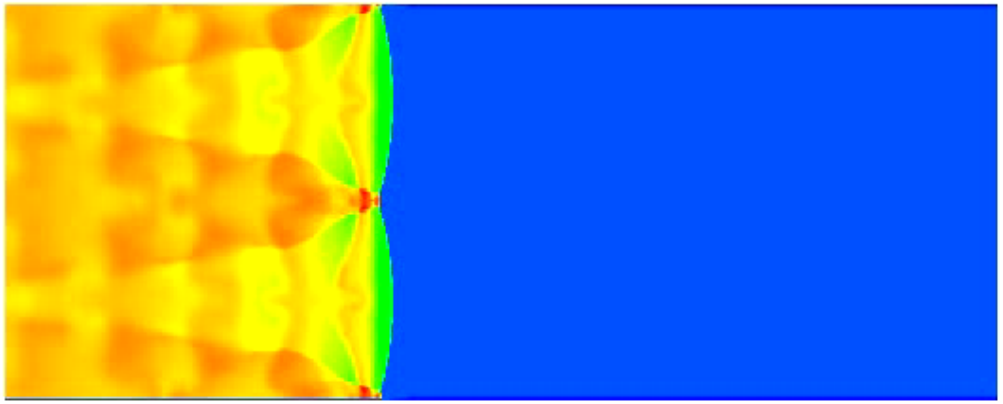

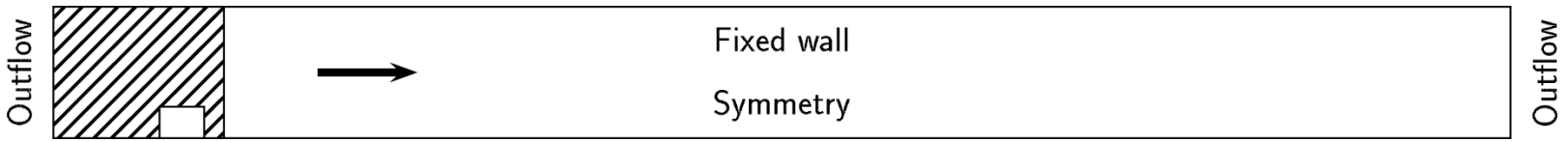

Simulation of regular cellular structures

- Regular Chapman-Jouguet detonation for $H_2 : O_2 : Ar/2 : 1 : 7$ at T_0 = 298K and p_0 = 10 kPa, cell width 1.6 cm.
- Perturb 1d solution with unreacted high-pressure pocket behind front
- Triple point trajectories by tracking max|ω| on auxiliary mesh

$$\omega = \frac{\partial u_2}{\partial x_1} - \frac{\partial u_1}{\partial x_2}$$

- Adaptation criteria:
  - *Scaled gradients of ρ and p*
  - *Error estimation in Y_i by Richardson extrapolation*
- 67.6 Pts within induction length. 4 additional refinement levels (2,2,2,4).
- Similar configuration as E. Oran et al., J. Combustion and Flame 113, 1998.

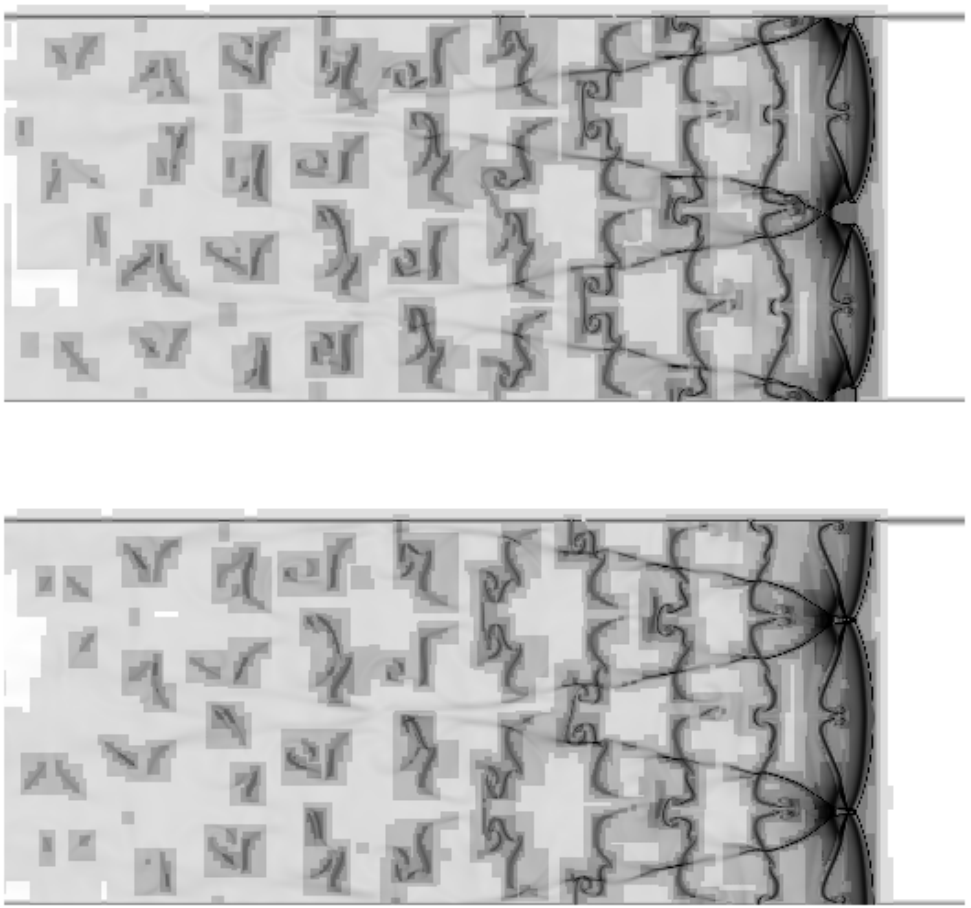

Flow Around a Triple-point

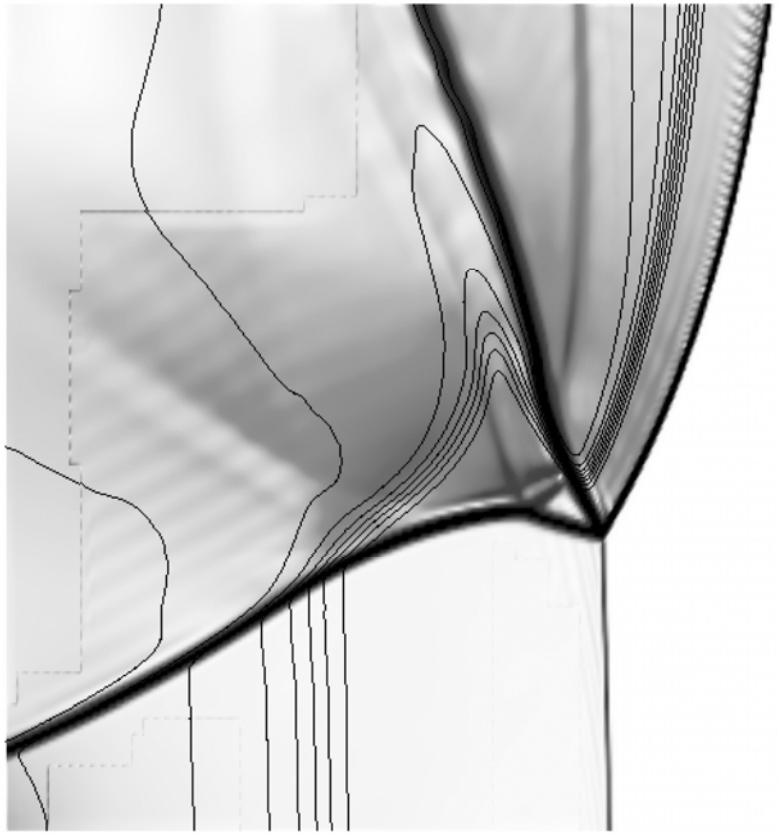

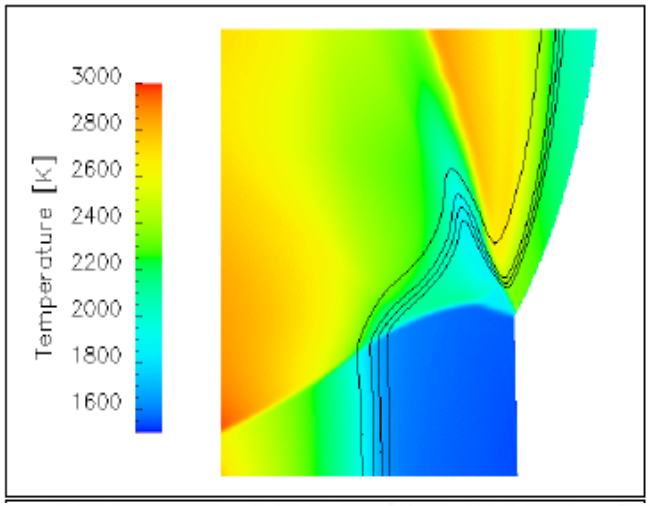

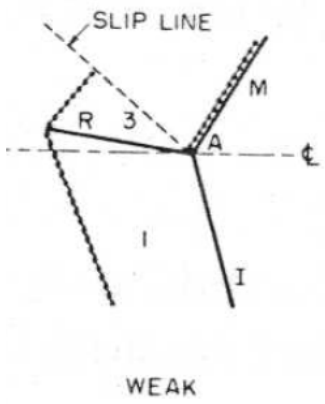

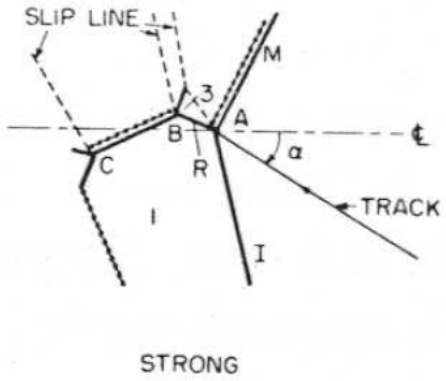

RD, Parallel adaptive simulation of multi-dimensional detonation structures, PhD thesis, BTU Cottbus, 2003

See also: Hu et al., The structure and evolution of a two-dimensional H_2/O_2/Ar cellular detonation, Shock Waves, 2004.

Flow Around a Triple-point

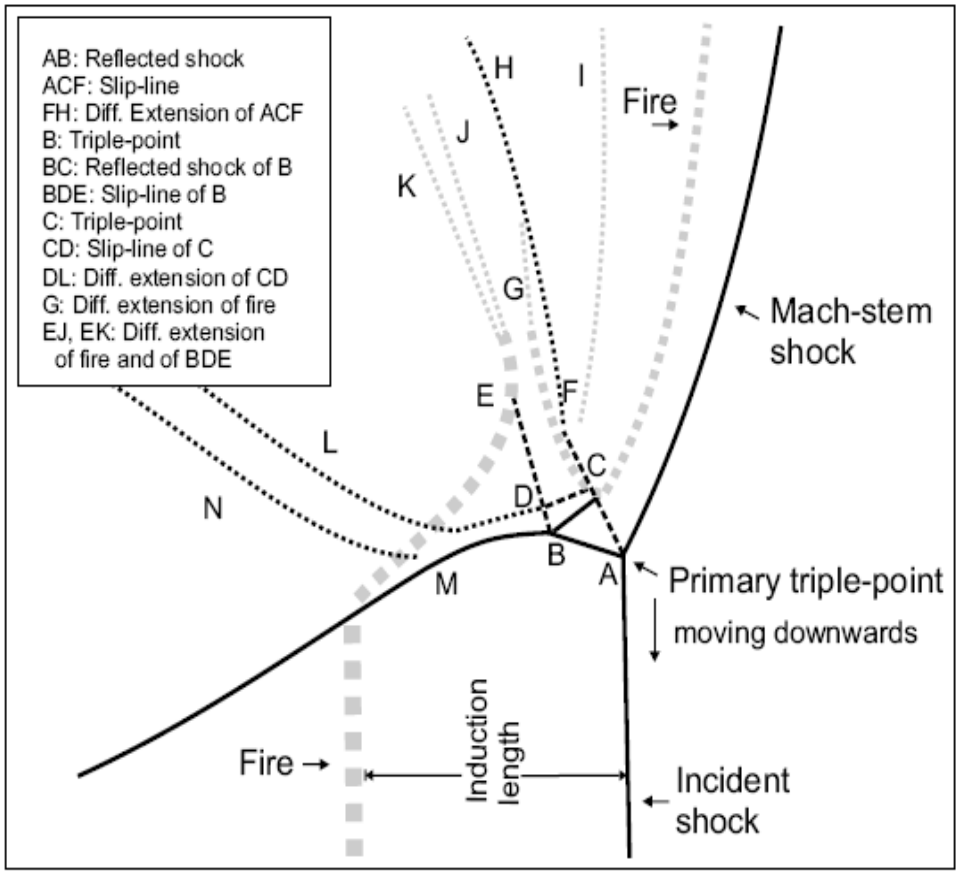

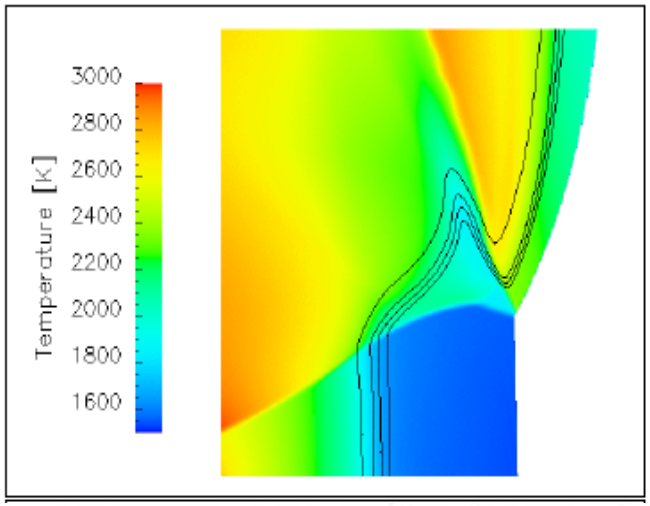

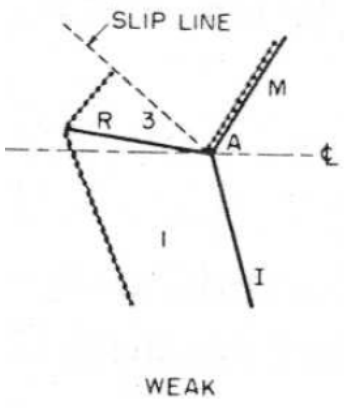

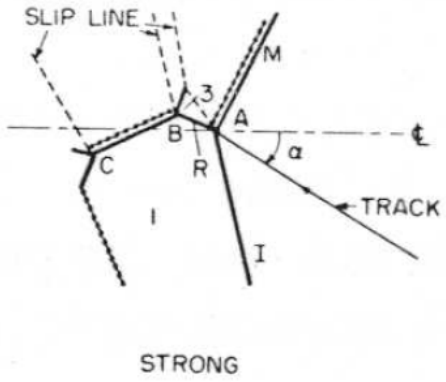

RD, Parallel adaptive simulation of multi-dimensional detonation structures, PhD thesis, BTU Cottbus, 2003

See also: Hu et al., The structure and evolution of a two-dimensional H_2/O_2/Ar cellular detonation, Shock Waves, 2004.

Oblique shock relations

Apply Rankine-Hugoniot condition $\sigma(\mathbf{q}-\mathbf{q}_0)=\omega\cdot(\mathbf{f}(\mathbf{q})-\mathbf{f}(\mathbf{q}_0))$ to steady shock wave with σ=0 described by the 2D Euler equations:

$$\begin{aligned}\rho_0 u_{0,n} &= \rho u_n \\ p_0+\rho_0 u_{0,n}^2 &= p+\rho u_n^2 \\ u_{0,t} &= u_t \\ h_0+\tfrac{1}{2}u_{0,n}^2 &= h+\tfrac{1}{2}u_n^2\end{aligned}$$

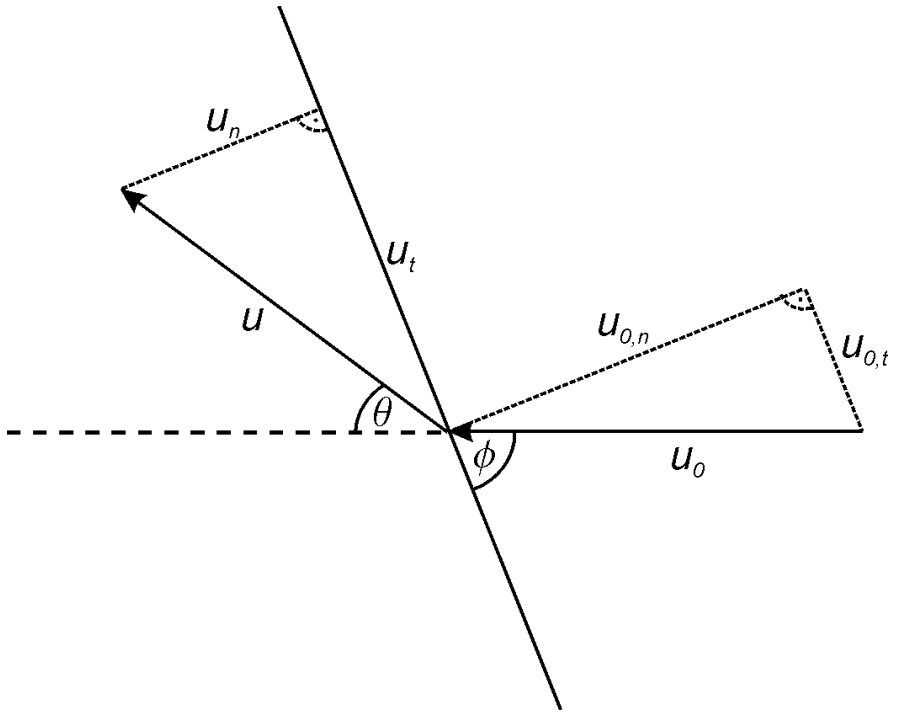

Commonly used:

$$\begin{aligned}\rho_0 u_0 \sin\phi &= \rho u \sin(\phi-\theta) \\ p_0+\rho_0 u_0^2 \sin^2\phi &= p+\rho u^2 \sin^2(\phi-\theta) \\ \rho_0 \tan\phi &= \rho \tan(\phi-\theta) \\ h_0+\tfrac{1}{2}u_0^2 \sin^2\phi &= h+\tfrac{1}{2}u^2 \sin^2(\phi-\theta)\end{aligned}$$

Oblique shock relations

Apply Rankine-Hugoniot condition $\sigma(\mathbf{q}-\mathbf{q}_0)=\omega\cdot(\mathbf{f}(\mathbf{q})-\mathbf{f}(\mathbf{q}_0))$ to steady shock wave with σ=0 described by the 2D Euler equations:

$$\rho_0 u_{0,n} = \rho u_n$$
$$p_0 + \rho_0 u_{0,n}^2 = p + \rho u_n^2$$
$$u_{0,t} = u_t$$
$$h_0 + \tfrac{1}{2}u_{0,n}^2 = h + \tfrac{1}{2}u_n^2$$

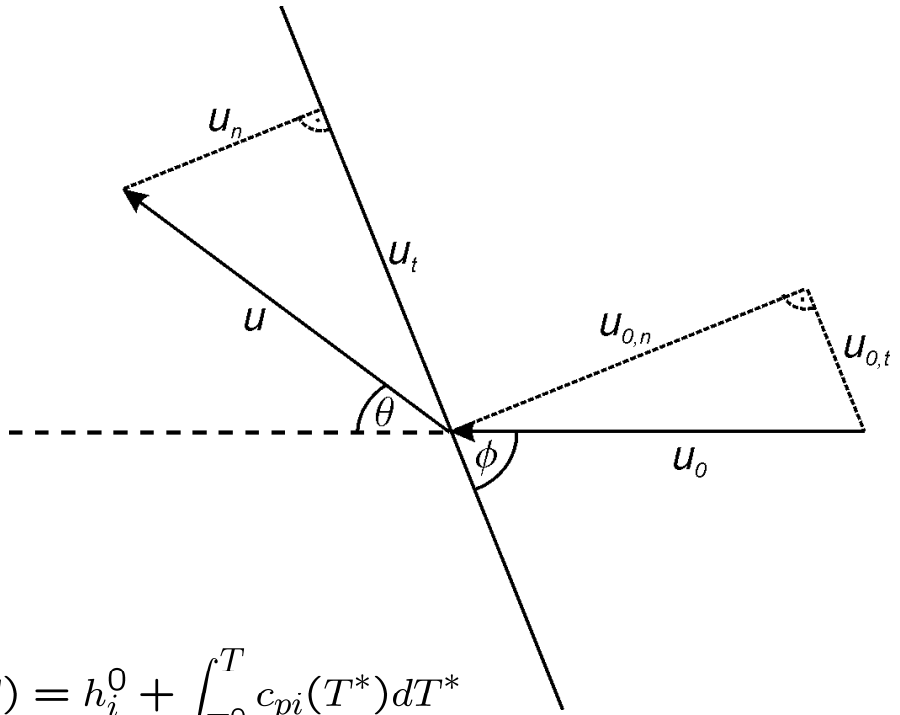

For thermally perfect mixtures with $h_i(T) = h_i^0 + \int_{T^0}^{T} c_{pi}(T^*)dT^*$ one solves

$$f(T) := \frac{RT_0}{u_{0,n}} + u_{0,n} - \frac{RT}{u_n} + u_n = 0 \quad \text{with} \quad u_n = \sqrt{u_{0,n}^2 - 2\int_{T_0}^{T} c_p(\nu)d\nu}$$

numerically

Triple point configurations & Transition criteria

- Irregular reflection (IR) to regular reflection (RR): $M_B{}^T$=1 with $M_B{}^T$>1 for RR

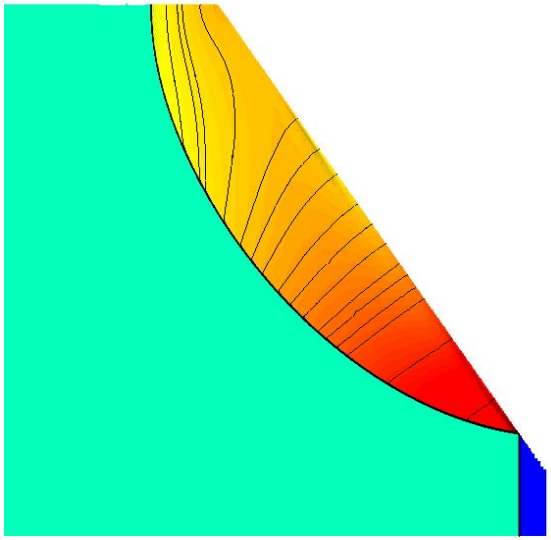

Triple point configurations & Transition criteria

- Irregular reflection (IR) to regular reflection (RR): $M_B{}^T$=1 with $M_B{}^T$>1 for RR

In the IR regime:

- von Neumann reflection (NR) to Mach reflection (MR): $M_D{}^T$=1 with $M_D{}^T$>1 for MR

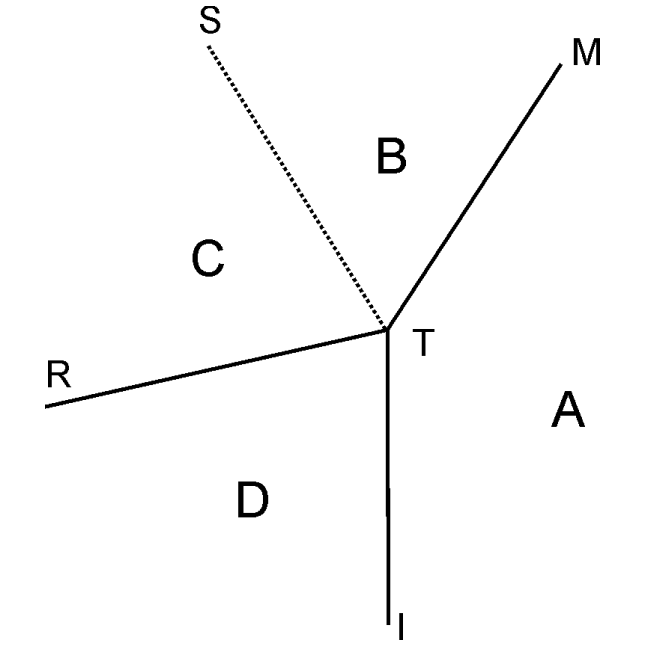

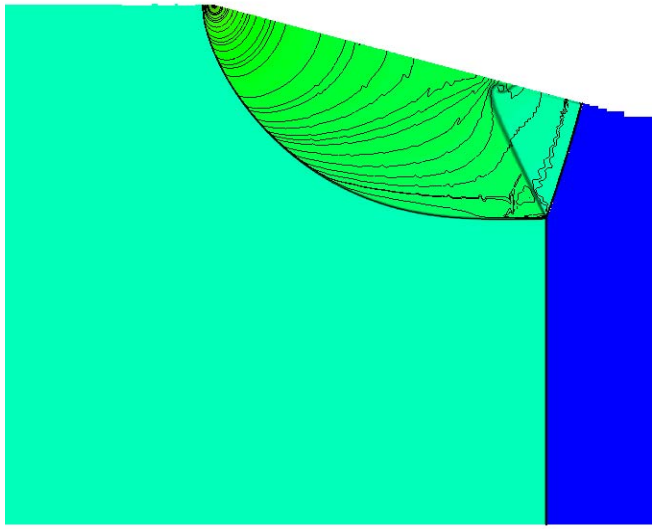

Triple point configurations & Transition criteria

- Irregular reflection (IR) to regular reflection (RR): $M_B{}^T$=1 with $M_B{}^T$>1 for RR

In the IR regime:

- von Neumann reflection (NR) to Mach reflection (MR): $M_D{}^T$=1 with $M_D{}^T$>1 for MR
- Single Mach reflection (SMR) to transitional or double Mach reflection (TMR/DMR): $M_C{}^T$=1 with $M_C{}^T$>1 for TMR/DMR

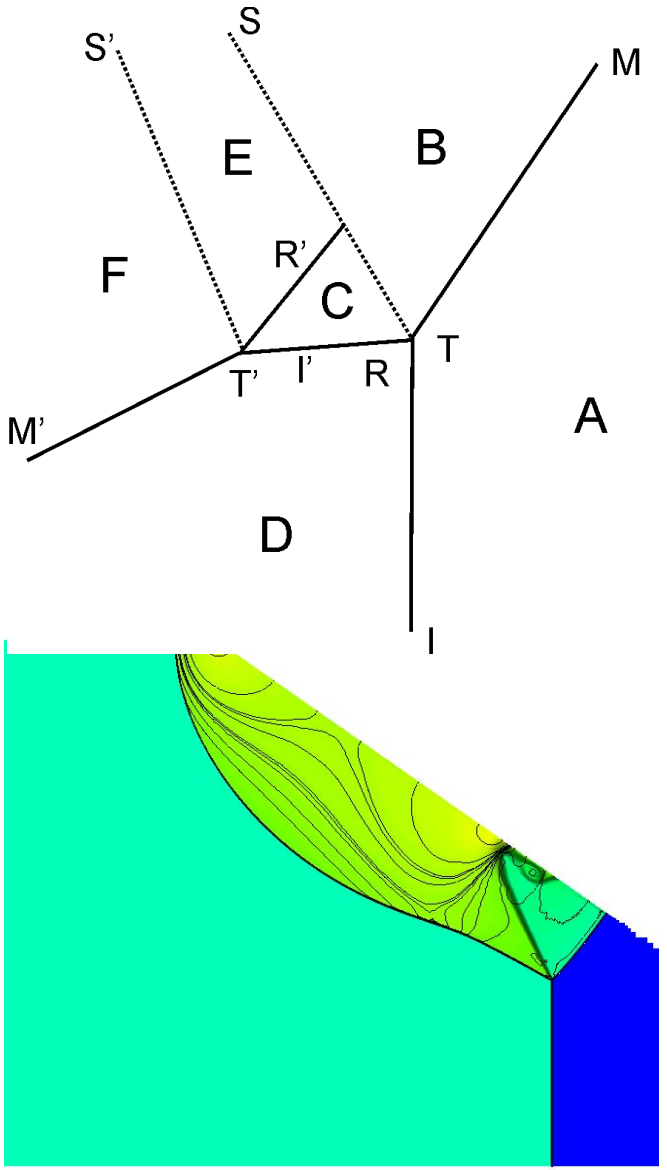

Triple point configurations & Transition criteria

- Irregular reflection (IR) to regular reflection (RR): $M_B{}^T$=1 with $M_B{}^T$>1 for RR

In the IR regime:

- von Neumann reflection (NR) to Mach reflection (MR): $M_D{}^T$=1 with $M_D{}^T$>1 for MR
- Single Mach reflection (SMR) to transitional or double Mach reflection (TMR/DMR): $M_C{}^T$=1 with $M_C{}^T$>1 for TMR/DMR
- Transitional (TMR) to double Mach reflection (DMR): $M_C{}^{T'}$=1 with $M_C{}^{T'}$>1 for DMR

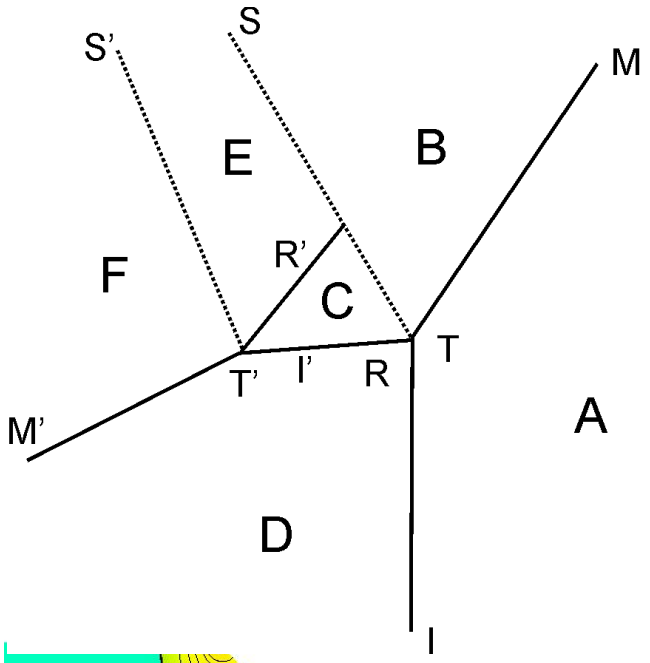

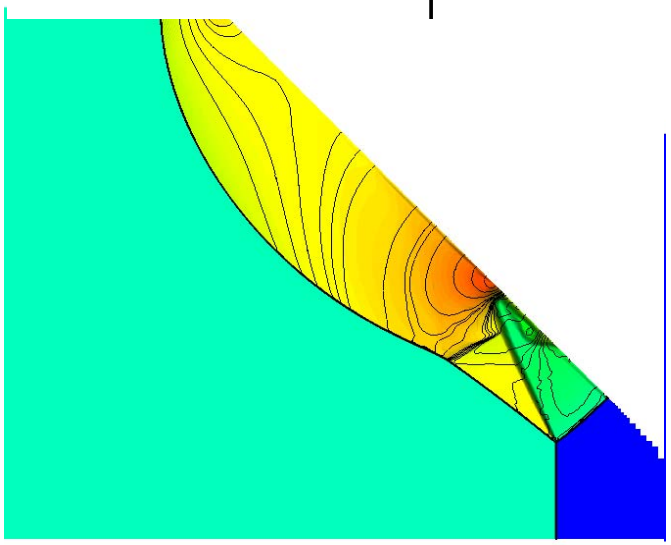

G. Ben-Dor, Shock wave reflection phenomena, 2nd ed., Springer, 2007.

Shock polar analysis for a DMR

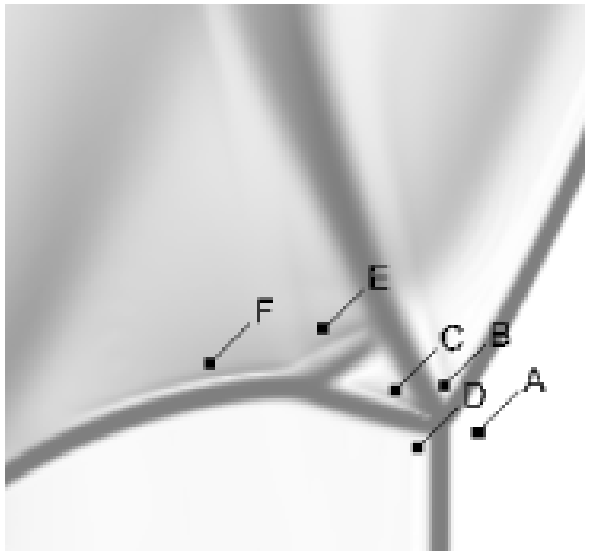

	p/p_0	r/r_0	$\mathbf{u}$[m/s]	α	γ	M	$\mathbf{u}'$[m/s]	α'	M'
A	1.00	1.00	1775	-39.5	1.557	5.078	1718	-40.2	4.916
B	31.45	4.17	447	-64.4	1.487	0.477	407	-70.3	0.433
C	31.69	5.32	965	-64.4	1.500	1.153	923	-67.0	1.103
D	19.17	3.84	1178	-73.2	1.509	1.533	1144	-75.7	1.488
E	35.61	5.72	901	-67.9	1.497	1.053	862	-70.8	1.007
F	40.61	6.09	777	-70.0	1.494	0.880	740	-73.6	0.838

$a_t \approx 60$ m/s used.

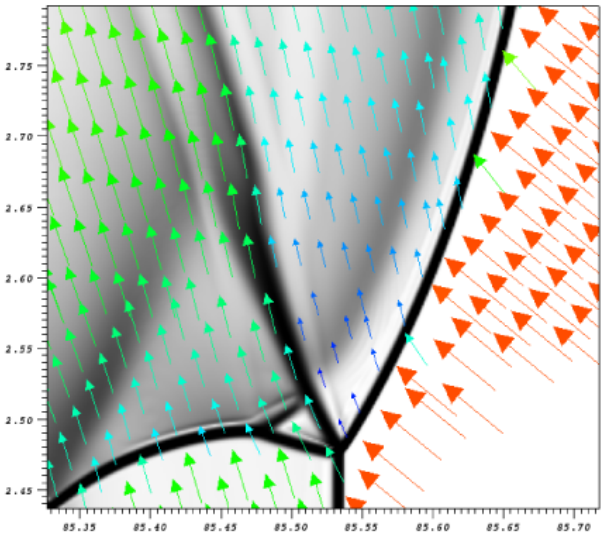

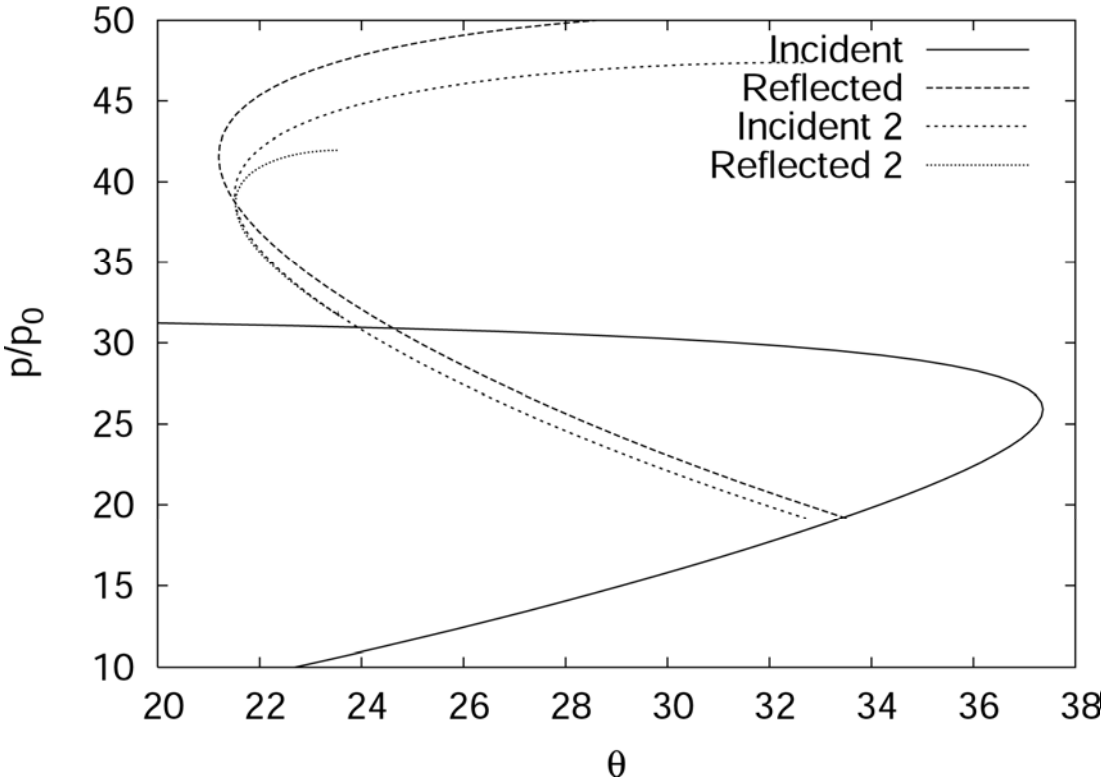

$\mathbf{u}'_C$=943 m/s used for plot (+2.2%)

Reflection types depending on transverse wave strength

$H_2 : O_2 : Ar/2 : 1 : 7$ at $T_0 = 298K$ and $p_0 = 10$ kPa

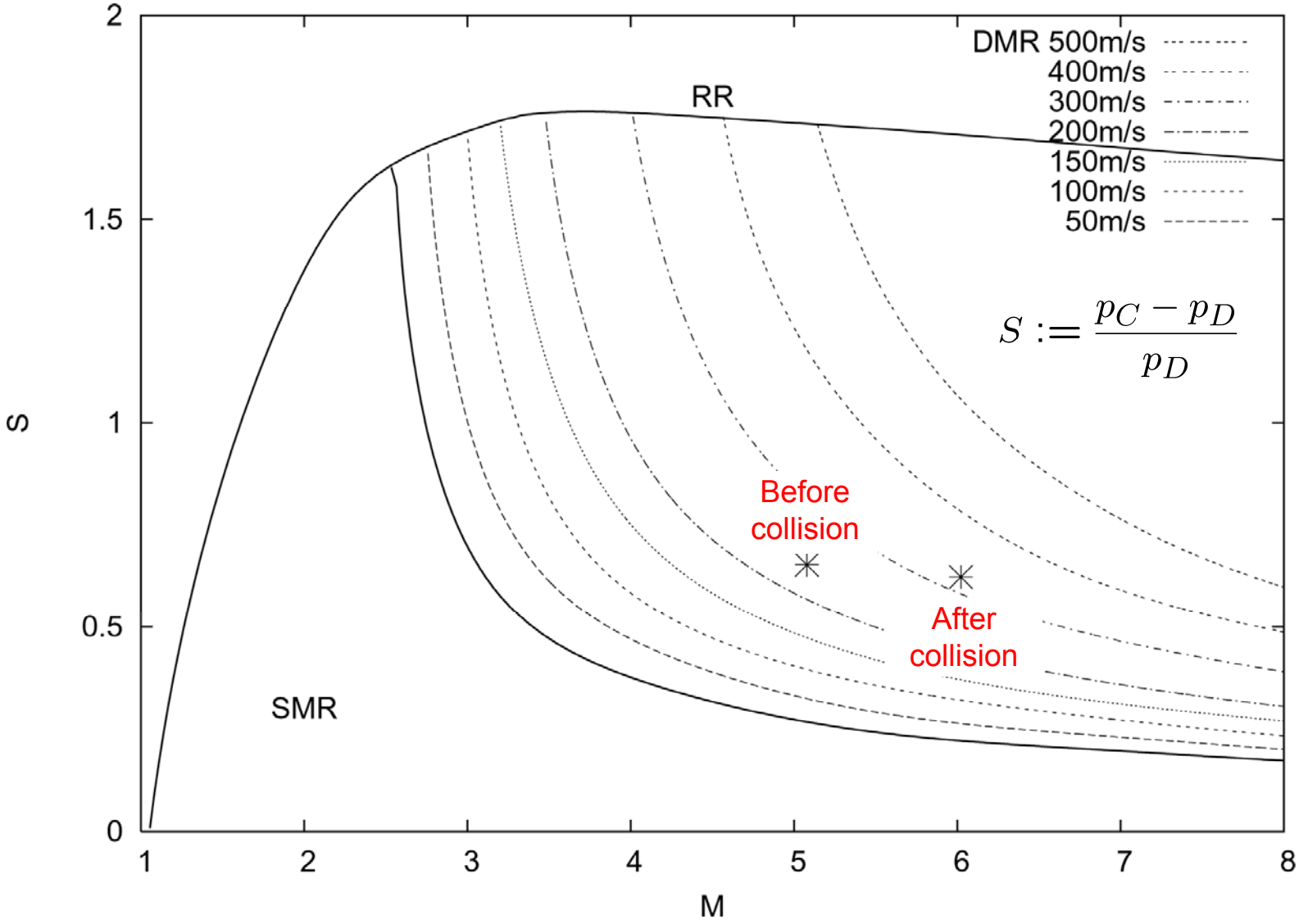

Transient conditions: Propagation through smooth pipe bends

- Regular Chapman-Jouguet detonation for $H_2 : O_2 : Ar/2 : 1 : 7$ at T_0 = 298K and p_0=10 kPa, cell width 1.6 cm, tube width of 5 detonation cells (8 cm)
- Pipe bend with same radius. Angle: 15^o, 30^o, 45^o, 60^o
- 56.2 Pts within induction length. 4 additional refinement levels (2,2,2,4)
- Adaptive computations use $\approx 7 \cdot 10^6$ cells ($\approx 5 \cdot 10^6$ on highest level) instead of $1.2 \cdot 10^9$ cells (uniform grid)
- ~70,000h CPU each on 128 CPUs Pentium-4 2.2GHz

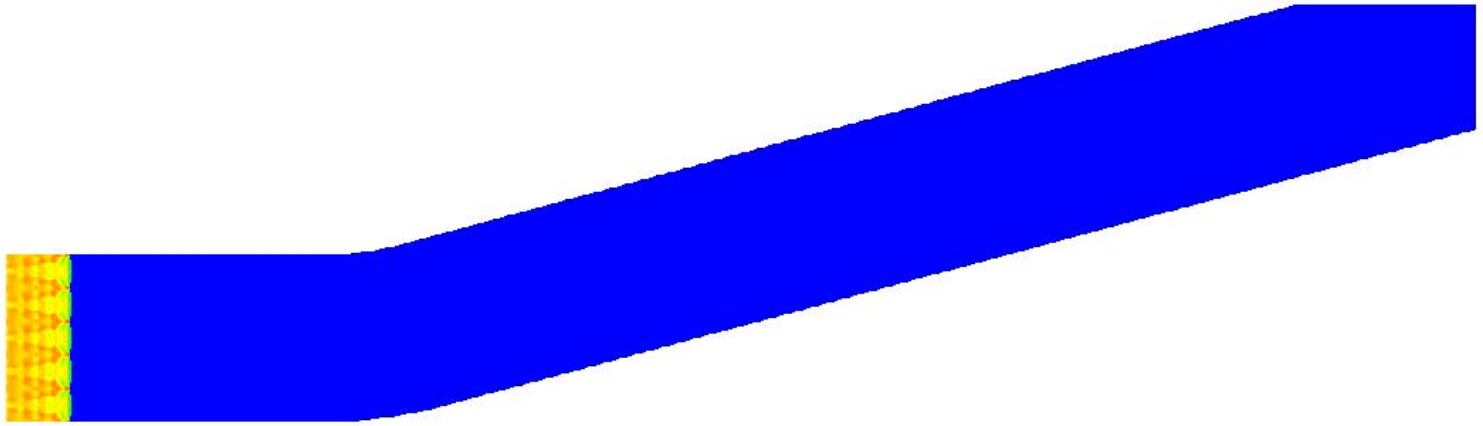

Color plot of temperature, 15^o pipe bend

Dynamic mesh adaptation (60º, 56.2 Pts/l_{ig})

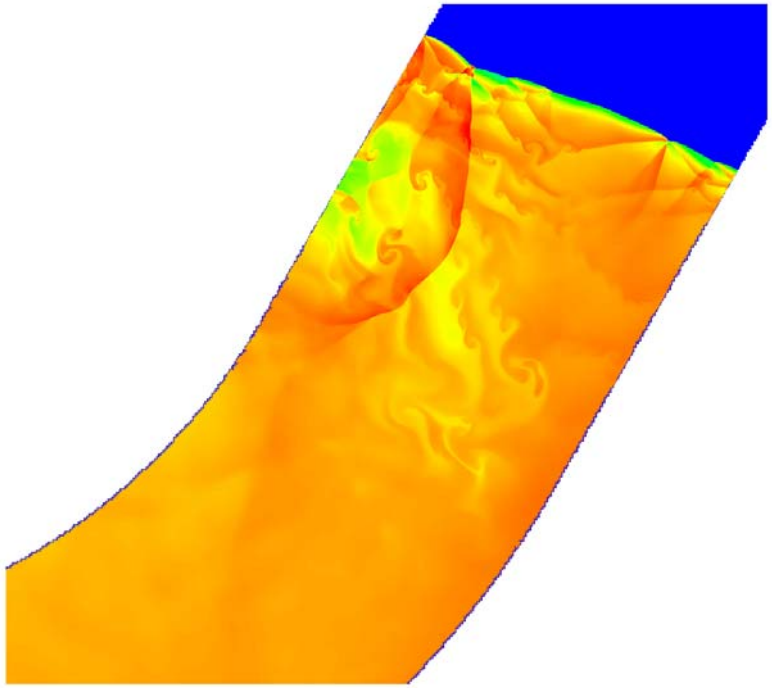

~170 μs

Time after entering bend

Enlarged triple point tracks (56.2 Pts/l_{ig})

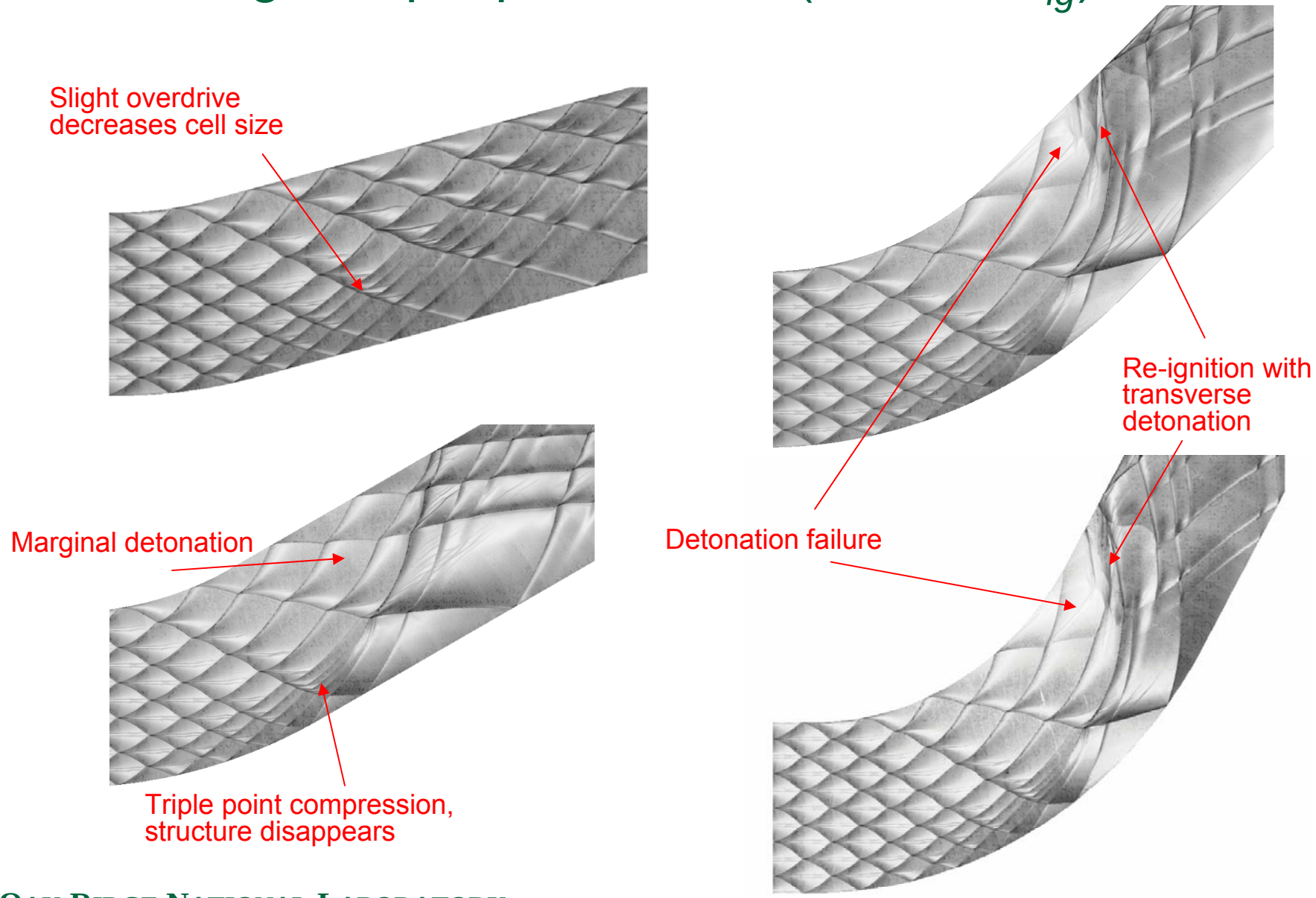

Resolution comparison (15°)– triple point tracks

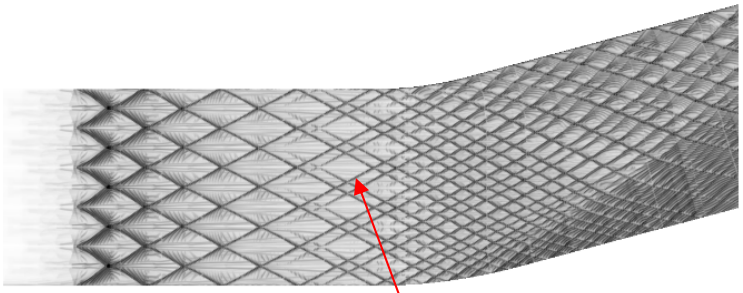

14.05 Pts/l_{ig}

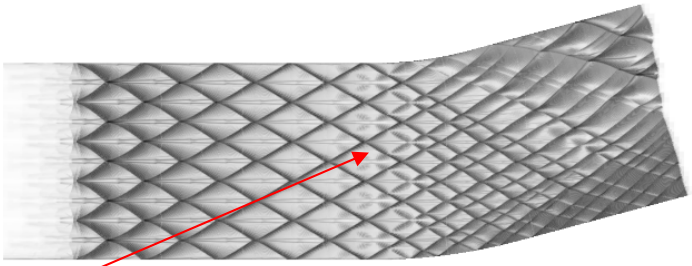

28.1 Pts/l_{ig}

Resolution insufficient to capture high-energy release in triple points

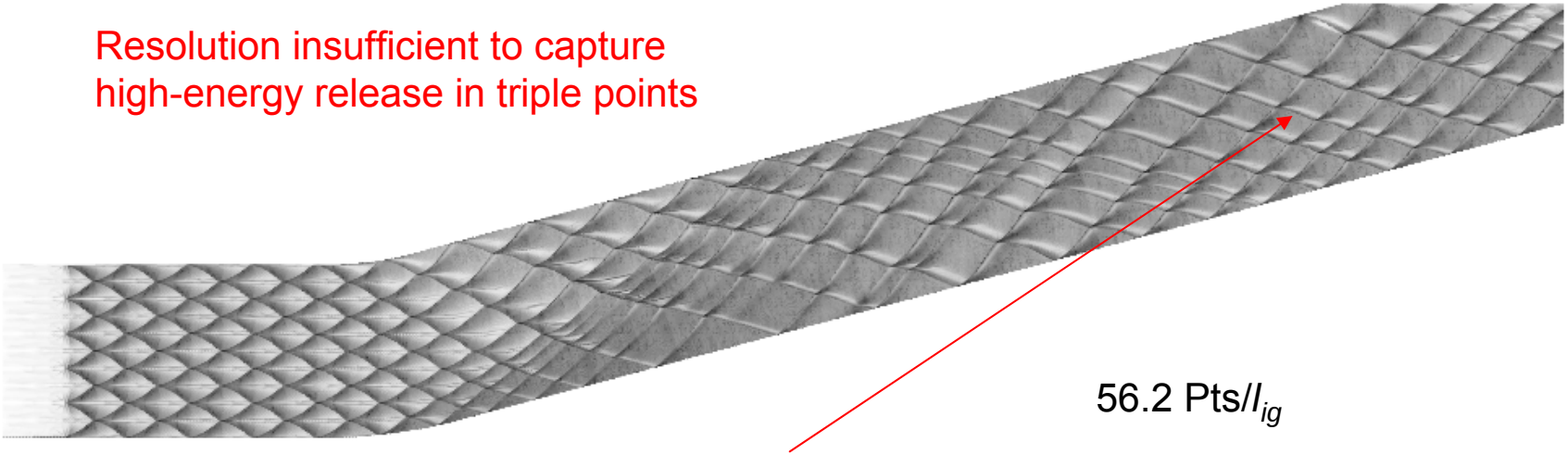

56.2 Pts/l_{ig}

Resolution sufficient: Number of triple points becomes approximately the same as before bend

Principal flow phenomena (45^0, 56.2 Pts/l_{ig})

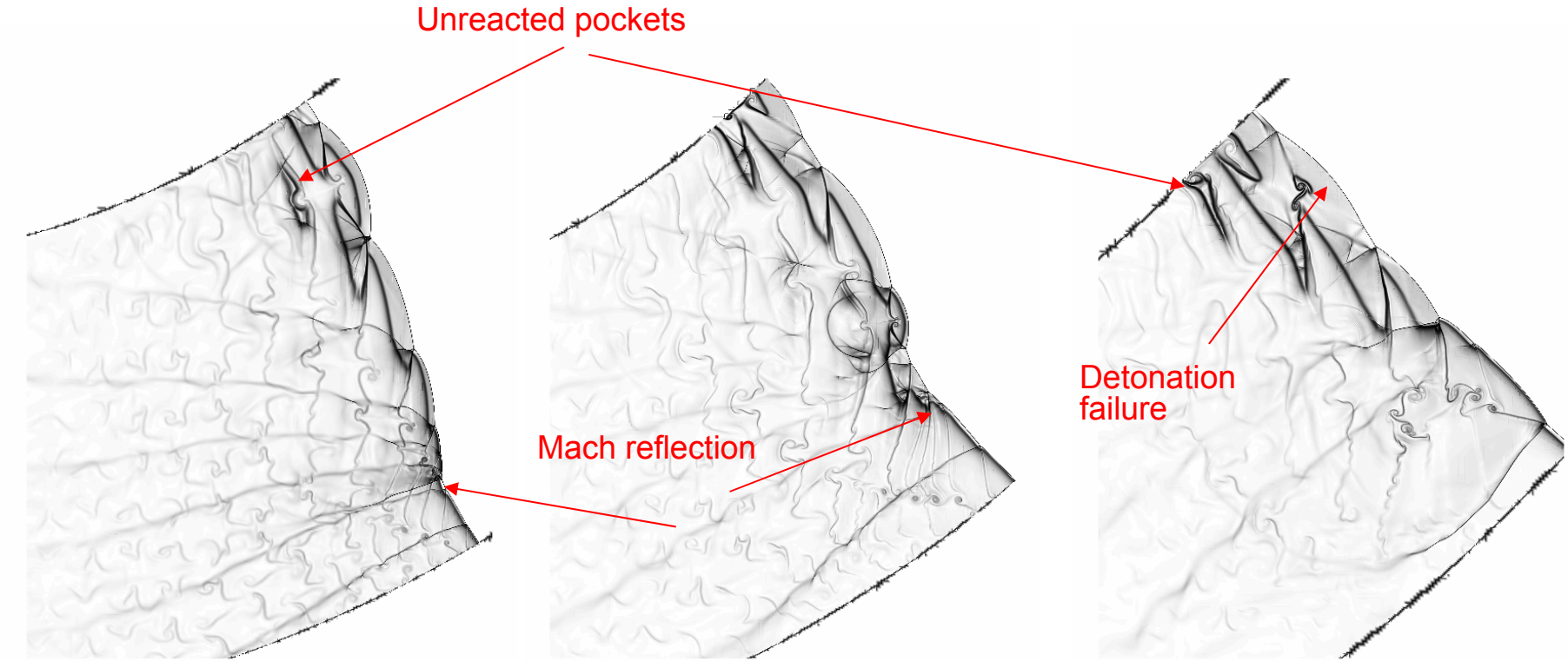

Principal flow phenomena (45^0, 56.2 Pts/l_{ig})

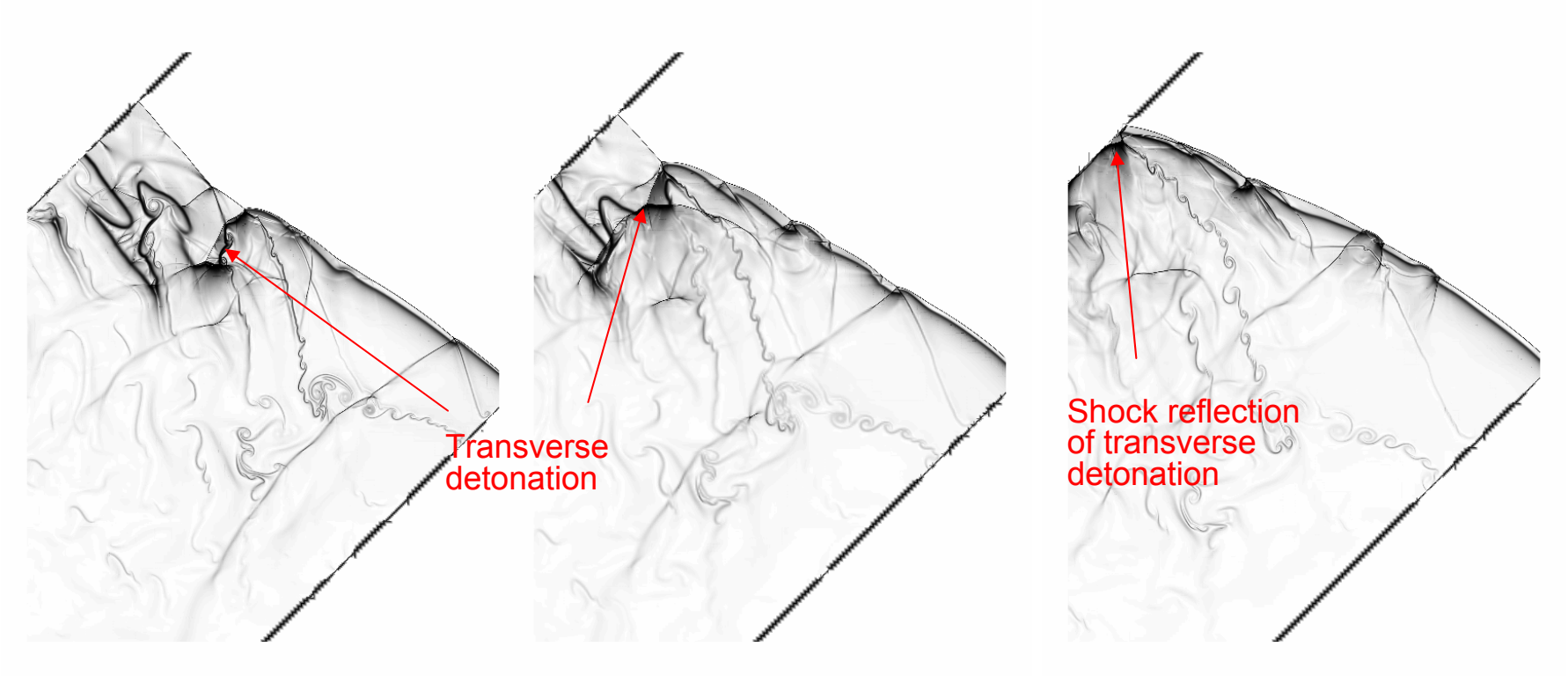

~120μs ~130μs ~140μs

Triple point analysis (15^0)

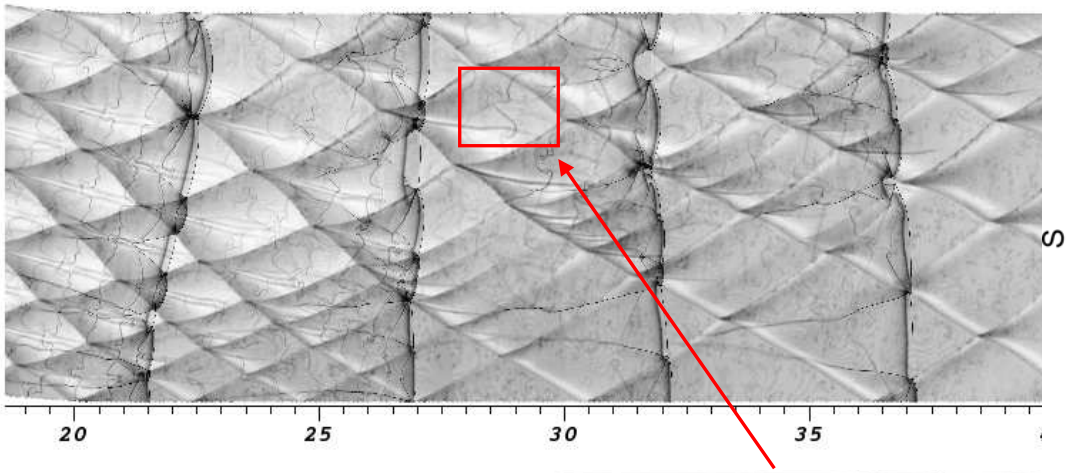

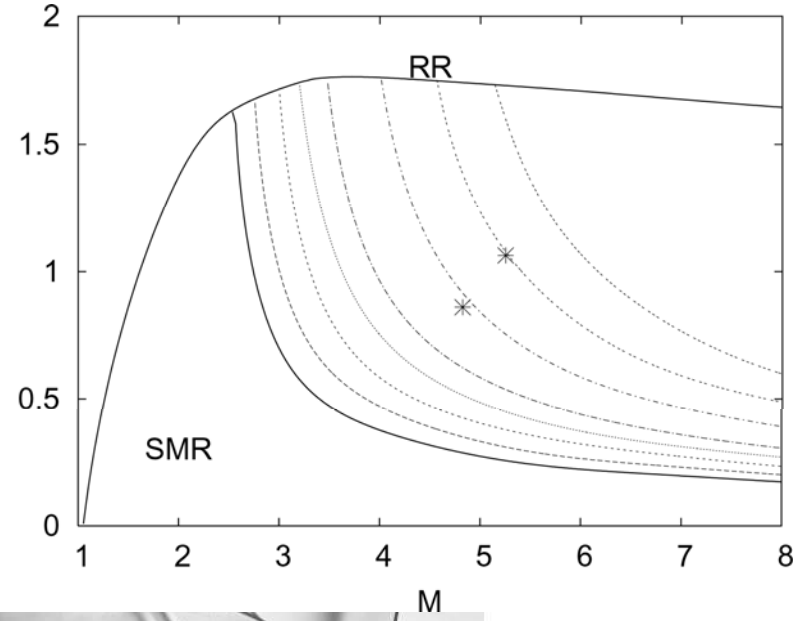

Strengthening of double Mach reflection pattern, trajectory angle increases

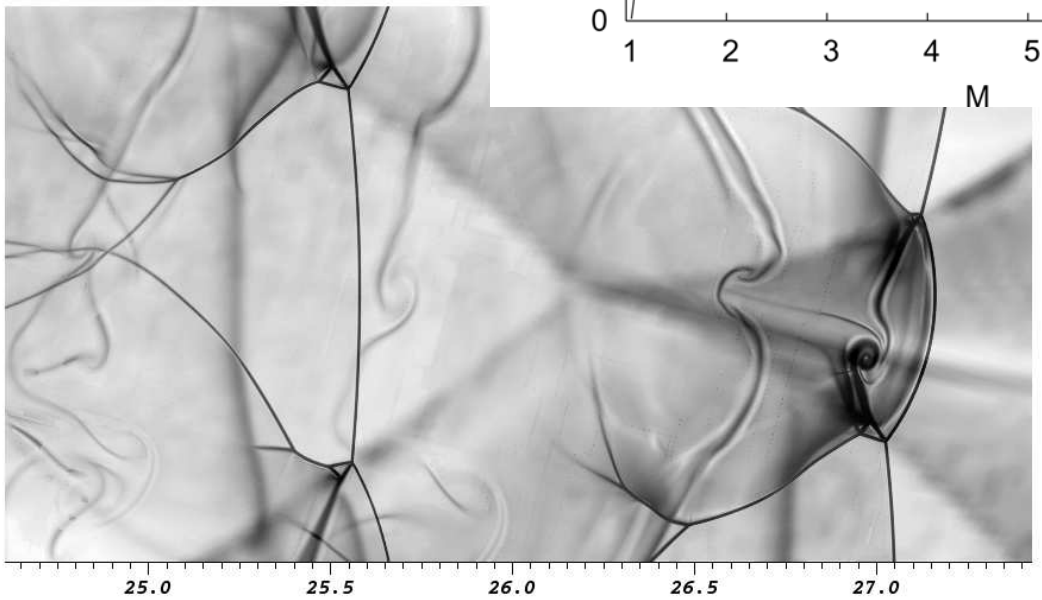

Triple point analysis (15^0)

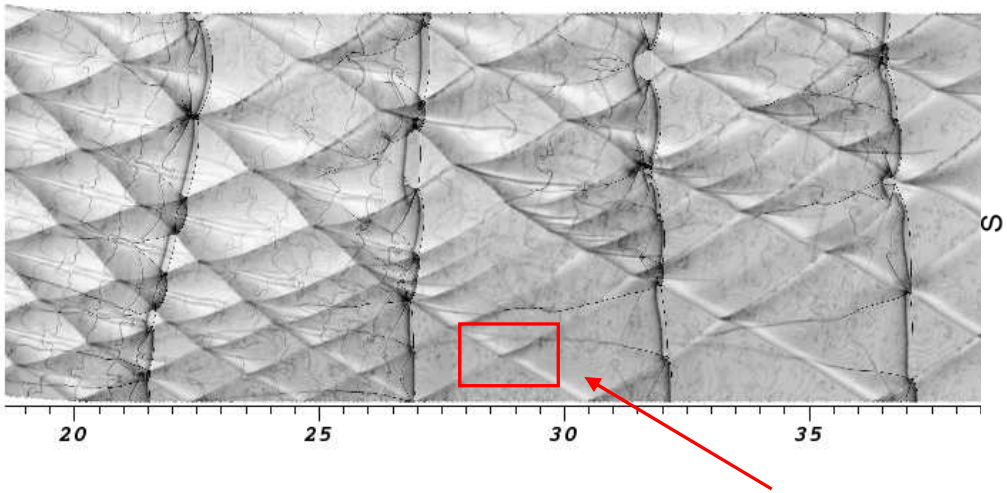

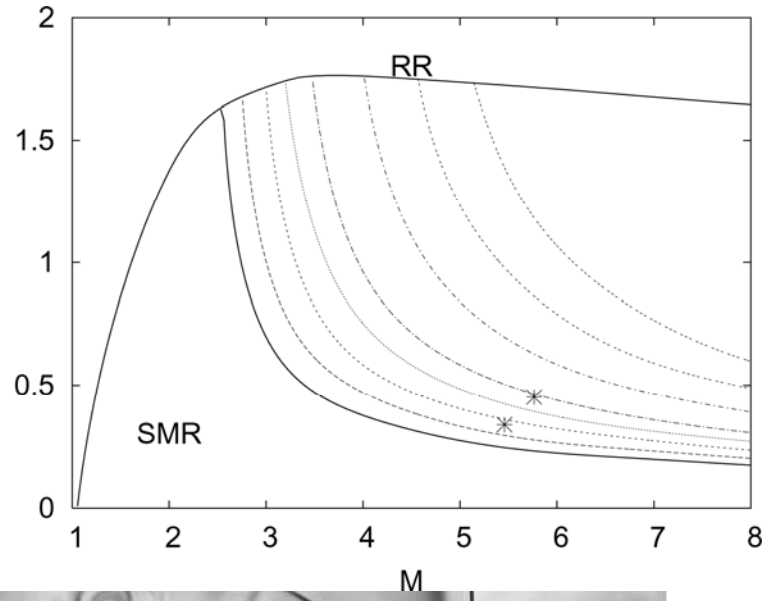

Transitional Mach reflection pattern,
Straight trajectories

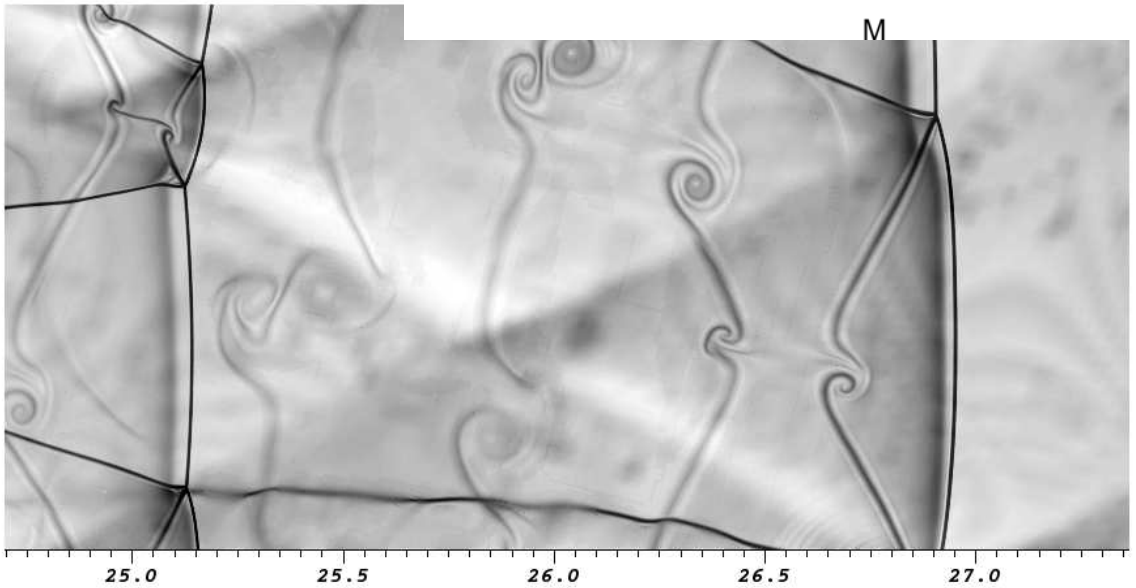

Triple point analysis (15^0)

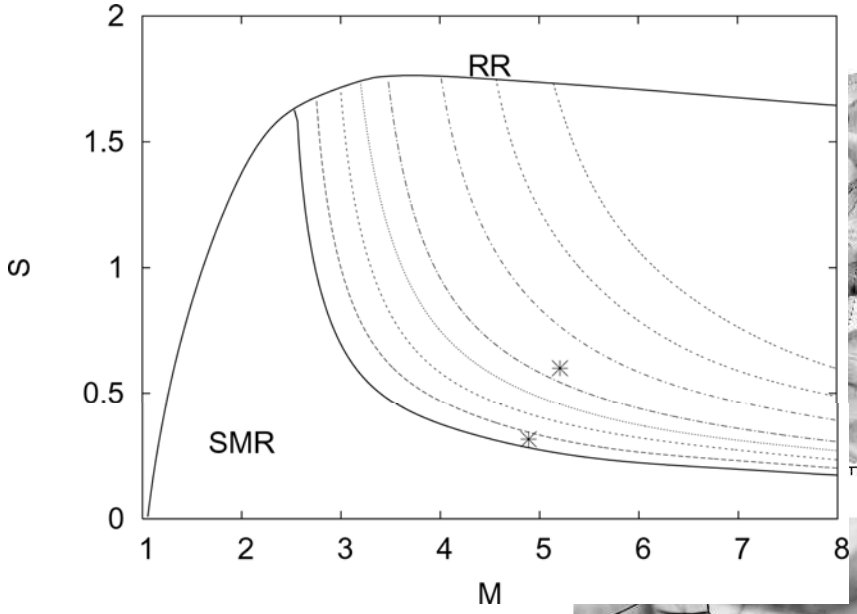

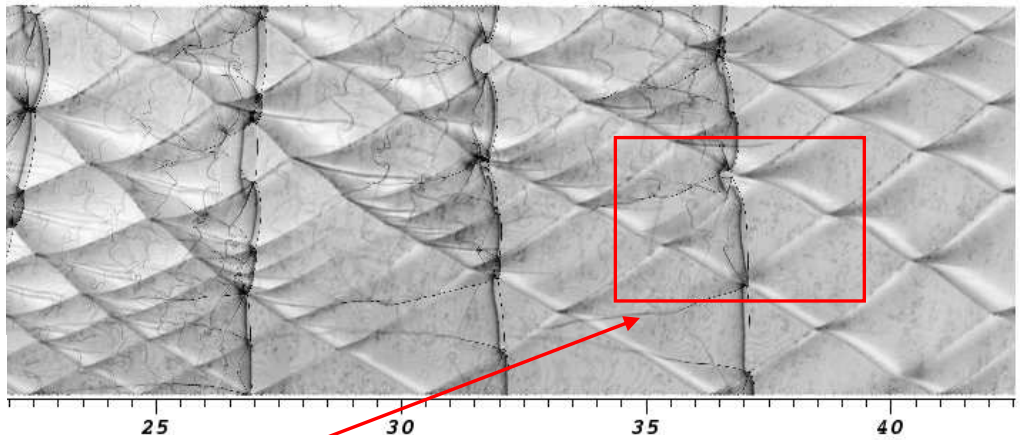

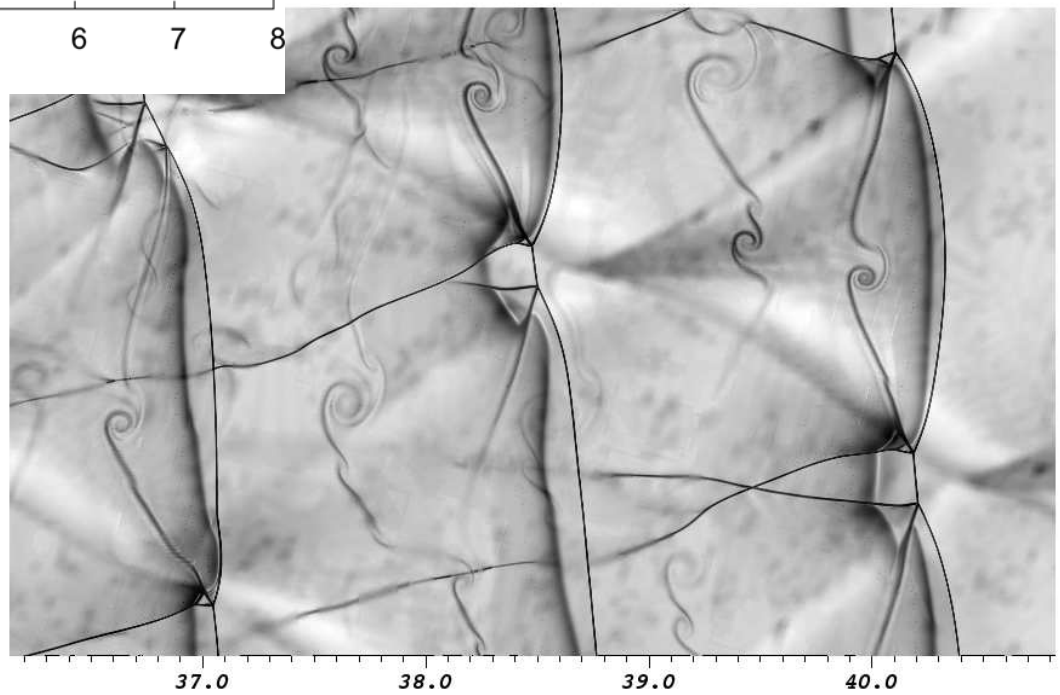

Formation of transverse wave with transitional Mach reflection, double Mach reflection after collision

Triple point analysis (30^0)

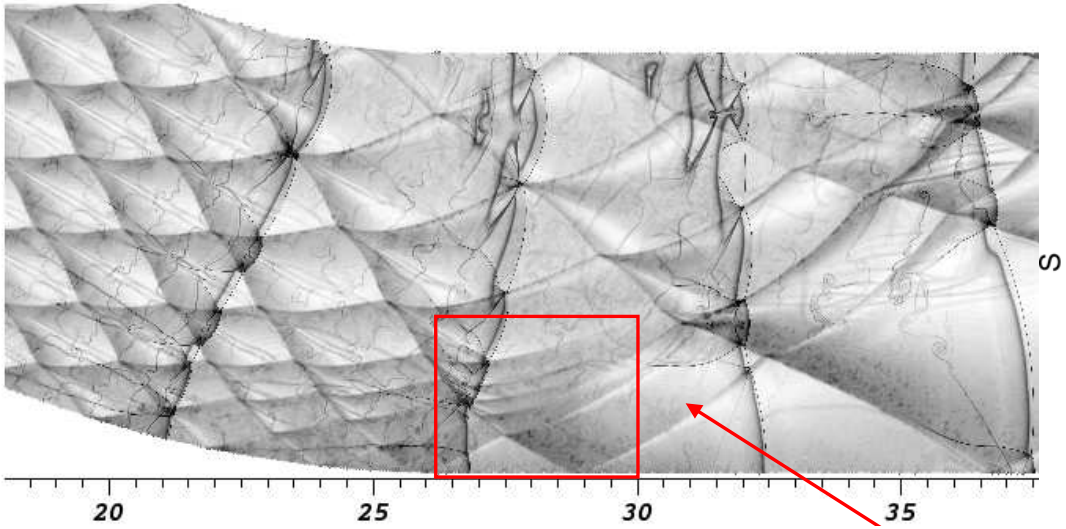

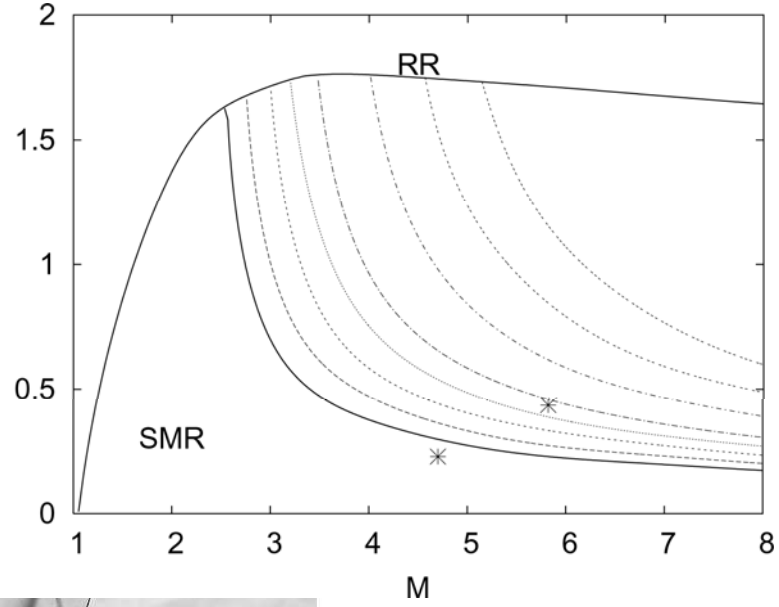

Triple point quenching and failure with weakening transitional Mach reflection patterns

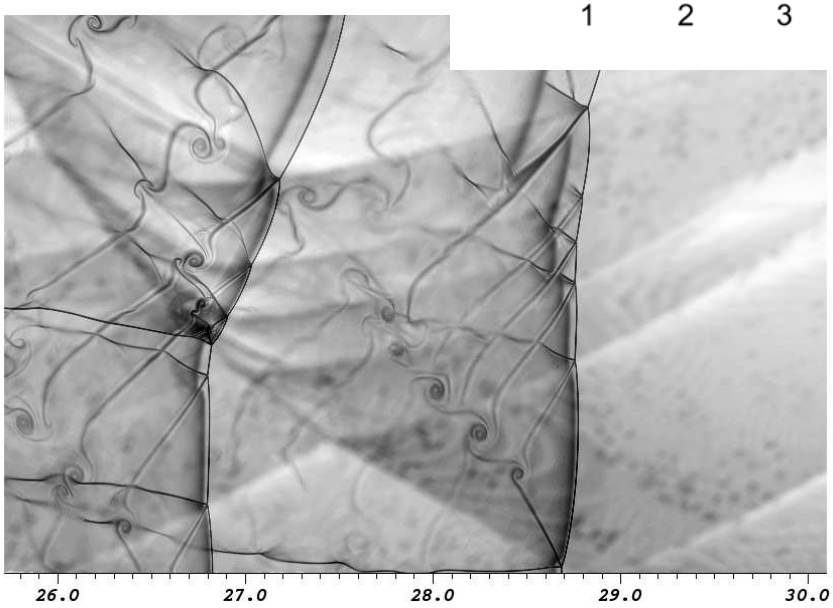

Triple point analysis (45^0)

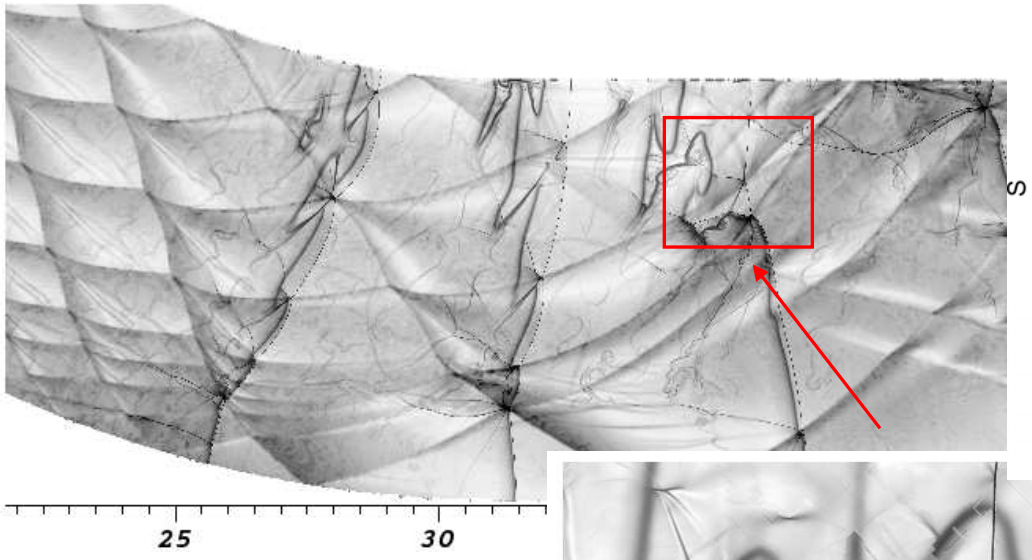

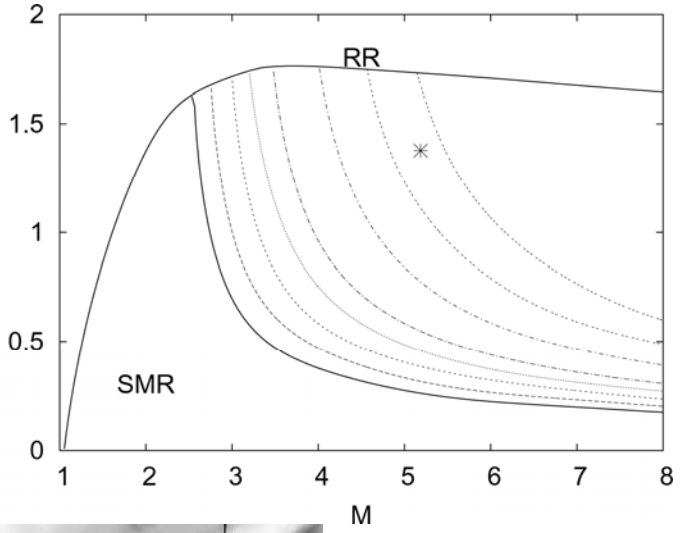

Transverse detonation with strong double Mach reflection pattern, triple point on transverse wave

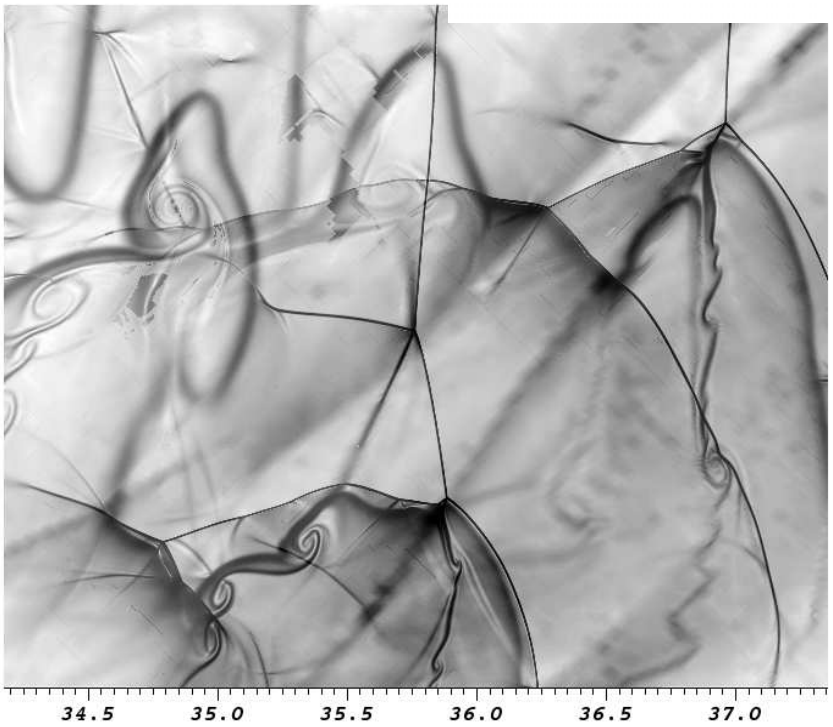

Outlook: Regular cellular structures in 3D

- Regular Chapman-Jouguet detonation for $H_2 : O_2 : Ar/2 : 1 : 7$ at T_0 = 298K and p_0=6.67 kPa, cell width 3 cm
- Unburned gas flows in with CJ velocity

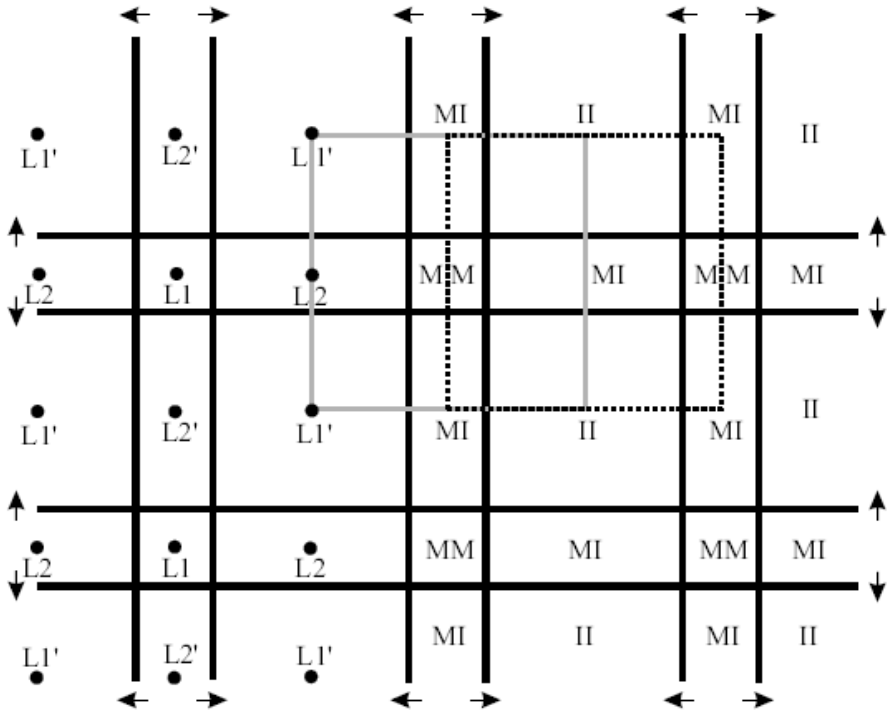

Front view of the periodic solution

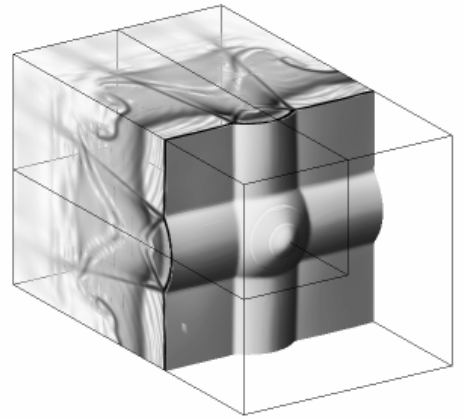

$t = 680\,\mu s + 600\,\mu s$ (Computation 1)

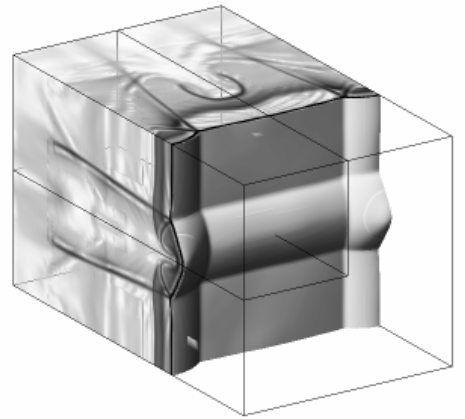

$t = 660\,\mu s + 620\,\mu s$ (Computation 2)

High-resolution simulation

- Simulation of only one quadrant
- 44.8 Pts within induction length
- AMR base grid 400x24x24, 2 additional refinement levels (2, 4)
- Simulation uses ~18M cells instead of 118M (unigrid)
- ~51,000h CPU on 128 CPU Compaq Alpha (LANL QSC)

Task	&
Fluid Dynamics	37.6
Chemical Kinetics	25.1
Boundary Setting	24.4
Reorganization	6.6
Misc.	6.3

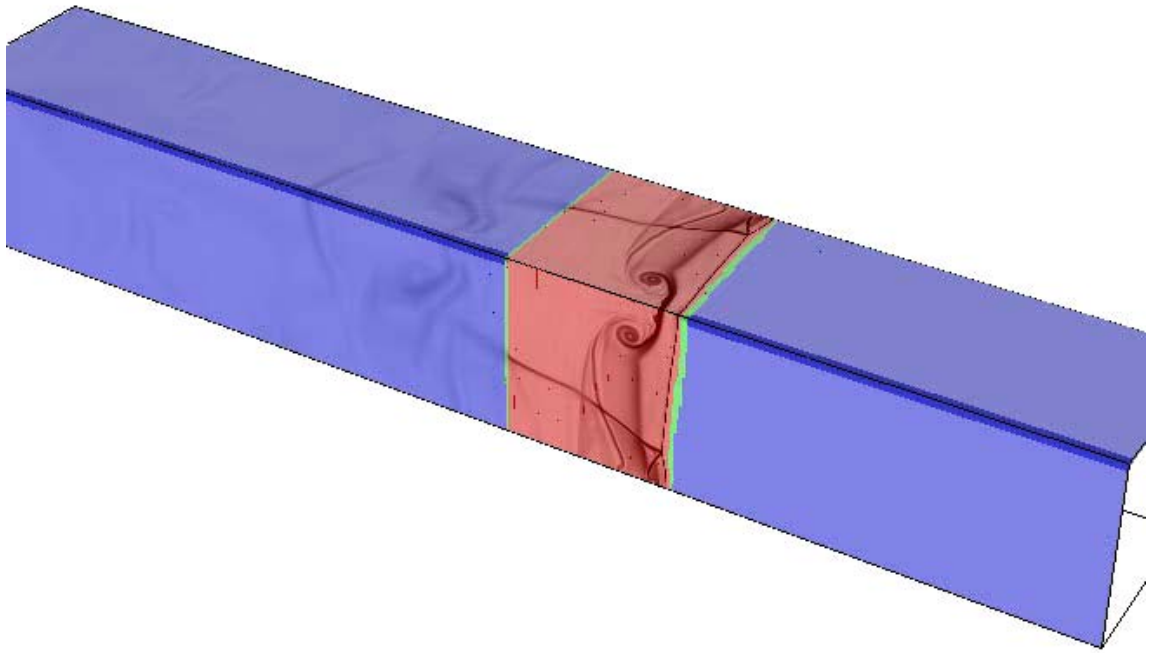

Schlieren plot of density of refinement domains

High-resolution simulation: Results

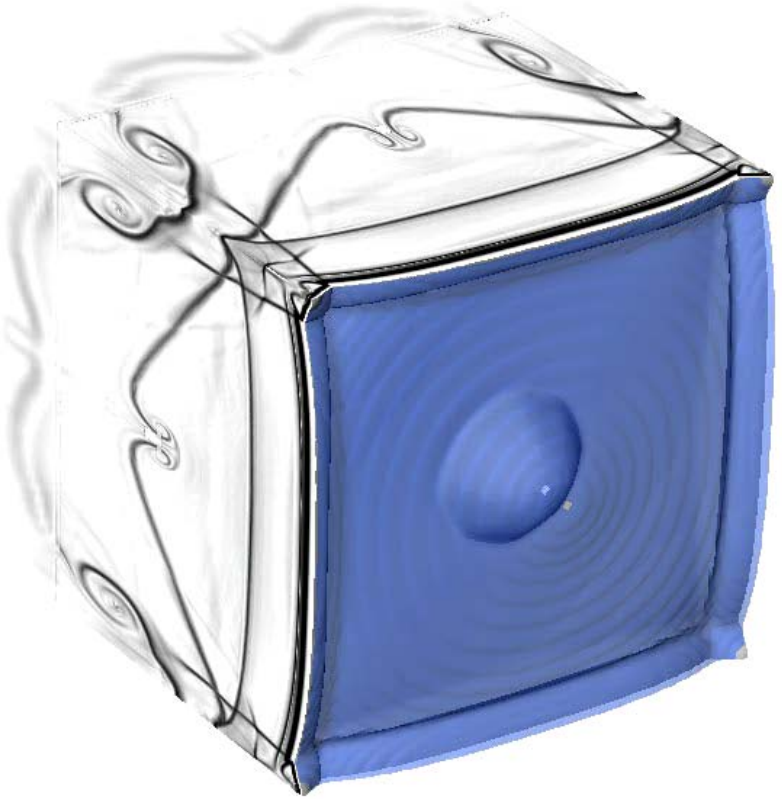

Schlieren plot of Y_{OH}, iso-surfaces of Y_{OH} and ρ visualize induction length, periodicity exploited for visualization

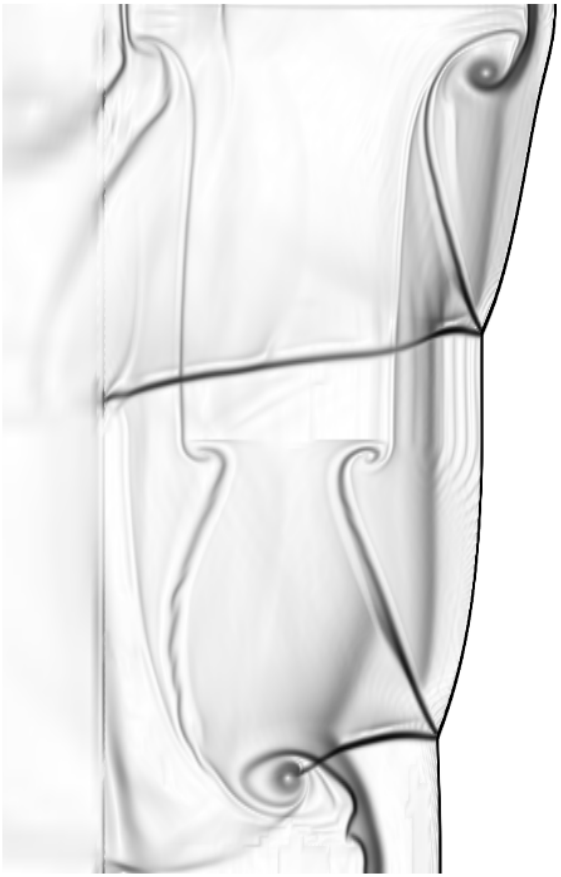

Transverse wave strength S smaller than in 2D. TMR patterns do occur!

Conclusions

- For particular mixtures, detailed detonation structure simulations with detailed chemistry are possible nowadays in 2D realistic geometries
- Accurate studies for idealized 3D configurations
- Resolution down to the scale of secondary triple points can be provided on parallel capacity computing systems
  - *Key components:*
    - *Operator splitting allows a cell-wise integration of stiff reaction terms*
    - *SAMR provides a sufficient spatial and temporal resolution, savings up to >250*
- Unreactive, thermally perfect shock polar analysis is applicable to explain observed reflection patterns
  - *Shock wave reflection theory is applicable to predict local triple point structure and stability*
  - *Triple point type is determined solely by S and M which can be derived from a single time step*
  - *Still missing: estimate for secondary triple point velocity a_t tailored for detonations to rigorously TMR/DMR transition*
- Observations:
  - *Stable triple point structures in self-sustained detonations seem to exist only in the TMR and DMR, but not in the SMR regime*
  - *A change of the reflection type happens especially in triple point collisions*
- Literature, links to software, papers, etc.: *http://www.csm.ornl.gov/~r2v*